

# Staleness Factor Model and Volatility Estimation

Xin-Bing Kong<sup>1</sup>, Bin Wu<sup>\*2</sup>, and Wuyi Ye<sup>2</sup>

<sup>1</sup>Southeast University, Nanjing 211189, China

<sup>2</sup>University of Science and Technology of China, Hefei 230026, China

October 11, 2024

## Abstract

In this paper, we introduce a novel nonstationary price staleness factor model allowing for market friction pervasive across assets and possible input covariates. With large panel high-frequency data, we give the maximum likelihood estimators of the regressing coefficients, and the factors and their loading parameters, which recovers the time-varying price stale probability and an integrated functional of the price staleness over two assets. The asymptotic results are obtained when both the dimension  $d$  and the sampling frequency  $n$  diverge simultaneously. With the local principal component analysis (LPCA) method, we find that the efficient price co-volatilities (systematic and idiosyncratic), are biased downward due to the presence of staleness. Bias corrected estimators of the systematic and idiosyncratic covolatilities (spot and integrated) are provided and proved to be consistent. Interestingly, beside their dependence on the dimensionality  $d$ , the integrated estimates converge with a factor of  $n^{-1/2}$  though the local PCA estimates converge with a factor of  $n^{-1/4}$ , validating the aggregation efficiency after nonlinear nonstationary factor analysis. But the bias correction degrade the convergence rates of the estimated (spot or integrated) systematic covolatilities. Numerical experiments justify our theoretical findings. Empirically, we observe that the staleness correction indeed leads to higher in-sample systematic volatility estimates, but a reduced out-of-sample portfolio risk almost uniformly in tested gross exposure levels.

**Keywords:** Staleness; High-frequency data; Continuous-time factor model; Large volatility matrix

---

\*Co-first and Corresponding author. Email: bin.w@ustc.edu.cn

# 1 Introduction

Price staleness refers to the phenomenon that asset prices are not updated as frequently as expected. One explanation is that it is caused by market friction that leads to sluggish price dynamics. As typically in absence of arbitrage opportunities, the asset price evolves as a semimartingale, and hence the path regularity demonstrates stochastic continuity. In particular, if the semimartingale is continuous driven by Brownian motions, the high-frequency returns shrink in square root of the time lag. However, the empirical evidence as in [Bandi et al. \(2017\)](#) shows that a large incidence of excessively small returns (smaller than a semimartingale implies) happen, demonstrating clear contradiction with semimartingale type behavior and indicating the presence of price staleness.

Staleness probability, statistically measured as the relative frequency of zero returns (zeros), is influenced by two primary factors: zero or near-zero trading volume and price discretization ([Bandi et al. 2020](#)). This concept provides valuable insights into the frictions within the trading process and their determinants (e.g., liquidity), making it crucial for understanding the asset price process and uncovering economic signals. Since [Bandi et al. \(2017\)](#) investigated into zeros using intraday data in a continuous-time setting, the literature on staleness has been starting to expand, c.f., [Kolokolov et al. \(2020\)](#), [Phillips and Yu \(2023\)](#), [Zhu and Liu \(2024\)](#). For ease of presentation, let  $t_j$  and  $t_{j-1}$  be two adjacent sampling times, a widely used model in theory and applications for the observed log price of an asset is as follows.

$$\tilde{Y}_{t_j} = Y_{t_j}(1 - B_{t_j}) + \tilde{Y}_{t_{j-1}}B_{t_j}, \quad (1)$$

where  $B_{t_j}$  is a Bernoulli random variable indicating the price updating depending on its value being one or zero. The second term is the sluggish price term depicting a likelihood that price staleness happens. The first term is an efficient price term and  $Y_t$  is a semimartingale as usual. But most studies focused on univariate series or multivariate processes of fixed dimension, while [Bandi et al. \(2024\)](#) found that the lack of price updating have a systematic component and thus pervasive across stocks. That being said, price staleness has cross-sectional correlation structure. It was also emphasized in the aforementioned works that zeros are as informative as volatilities and heavily detrimental for reliable inference on the efficient price dynamics like the volatility. Therefore, understanding and properly modeling the joint dynamics of the price stale probability of a large pool of assets are of vital importance in statistical theory and financial

applications.

To the best of knowledge, so far there isn't any paper on modeling the large-dimensional price staleness across high-dimensional asset price processes with large panel high-frequency data. This is a first motivation of the present paper. The rare paper [Bandi et al. \(2024\)](#) only gives a motivational study for the existence of price co-staleness and proposed statistical indicators to measure and explain the empirical patterns. Yet they assume that zero (or near-zero) returns occur simultaneously across all assets at each time stamp which is restrictive. In reality, there may be delays in the transmission of illiquid information across assets though contemporary occurrence probability of stale prices for all assets is positive, and simultaneous zeros for all assets are rare, especially at high frequencies for high-dimensional price processes. They also assumed that the systematic staleness is constant and driven by only one factor, which is not flexible enough. As shown in [Figure 1](#), the principal components of cross-sectional staleness for an intraday pattern demonstrate clear time variation. Systematic staleness is influenced by multiple factors, with the first factor accounting for only 35.9% of the variation and the first six factors cumulatively explaining about 76.8% of the total variation.

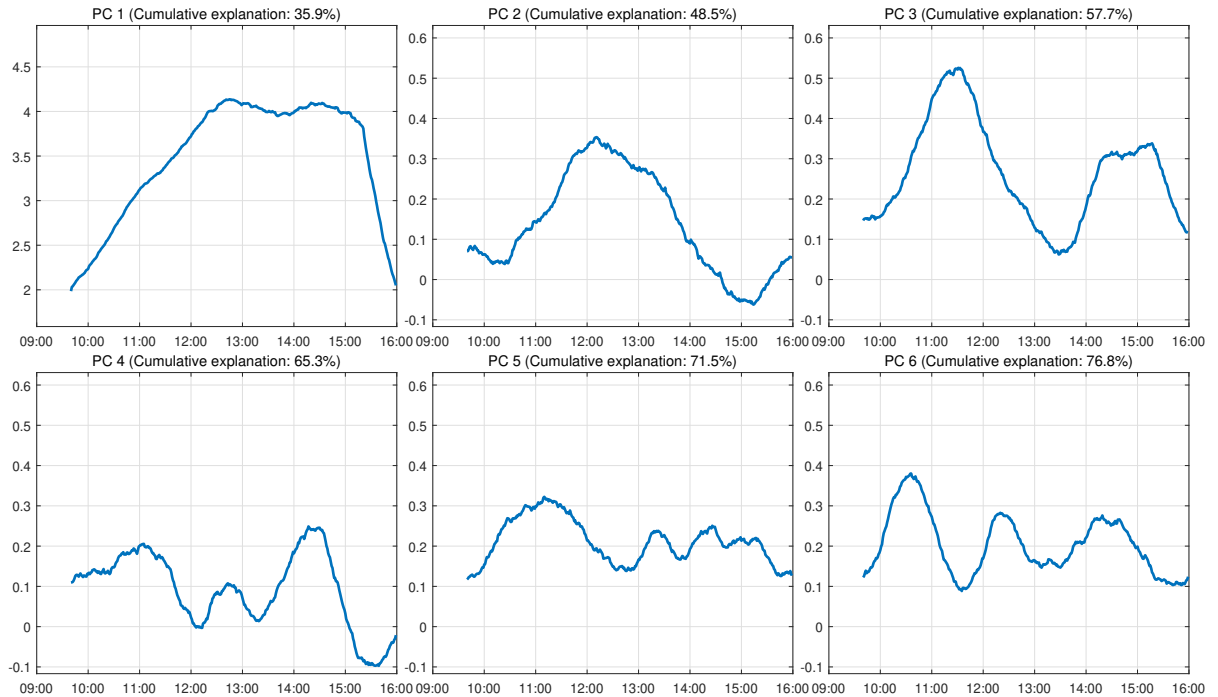


**Figure 1:** Principal components of intraday cross-sectional staleness. *Notes.* These graphs display the first six principal components extracted from the average intraday staleness of 152 stocks in March 2014. Each graph also includes the cumulative percentage of variation explained by the corresponding principal component. Spot staleness was estimated using the localized block method.

In this article, we formally introduce a novel nonlinear continuous-time model for high-dimensional staleness process, termed the staleness factor model (SFM). The model maps ex-

ogenous covariates and unobservable factors using a general link function (e.g., logit or probit). We set the covariates and factors as general Itô semimartingales, which are generally nonstationary. There are several merits of this model. First, via the link function and modeling a function of staleness probability with covariates and common factors, it is natural to explain the price-stale pervasiveness. Even common flat prices are not observed across all assets, the probability does not vanish making delayed flat price arrivals interpretable. Moreover, how the probabilities differ for distinct assets is clearly characterized by the price staleness factors. Second, the price-stale factors and even the covariate processes are allowed to be time-varying and thus more flexible and empirically supported. The resulting high-dimensional price trajectory is a superposition of a high-dimensional Brownian semimartingale and a high-dimensional Bernoulli process counting the zero high-frequency returns with the law of the high-dimensional staleness factor model, see Section 2.1 for details. Based on this model, we can analyze the systematic staleness factors in a large cross-section and the influence of exogenous variables. Besides the nonlinearity, a great difference with existing continuous-time factor models, such as those in Ait-Sahalia and Xiu (2017), Pelger (2019), and Kong (2017, 2018), is that the multivariate factor process as well as the price stale probability process are in their integrated form and can not be differenced because the price staleness probability (the probability that  $B_{t_j} = 1$ ) can not be observed. This causes challenge to the inference since the high-frequency global principal component analysis (GPCA) and the local principal component analysis (LPCA) methods (Kong et al. 2023) taken on differenced semimartingales are not applicable any more. This is tackled in the present paper. To estimate the nonlinear nonstationary staleness factor model, we employ a maximum likelihood estimation (MLE) procedure. We examine the asymptotic properties of the estimators when the dimension  $d$  and sample size  $n$  approach infinity. The estimator of the staleness probability has an error bound of order  $\min(\sqrt{n}, \sqrt{d})^{-1}$ , while the integrated version achieves the accuracy of order  $n^{-1/2}$ , consistent with the efficiency rate of the estimated volatility functionals theoretically underpinned in Jacod and Rosenbaum (2013). Notably, our estimator does not suffer from biases due to nonlinearity, volatility of volatility, and edge effects associated with aggregating the local estimates of staleness.

High-dimensional volatility matrix estimation is crucial for constructing large portfolios, risk management, pricing financial instruments, and estimating risk premiums for various risk factors. Natural questions under the framework of our newly proposed model arise. A first fundamental problem, with the superpositioned price staleness factor model making the semi-

martingale property biased, is how to estimate the efficient price volatility matrix contributed by the semimartingale component? A second interesting question is what is effect of the price staleness on the estimated efficient price volatilities (systematic and/or idiosyncratic)? The present paper aims at answering these questions. The first estimator of large sparse volatility matrix using high-frequency data was introduced by Wang and Zou (2010). This estimator has been refined and extensively studied by Tao et al. (2013) and Kim et al. (2018). Improved estimation can be achieved by imposing a low-rank plus sparse structure (e.g., Ait-Sahalia and Xiu 2017; Kong 2018; Fan and Kim 2018, 2019; Dai et al. 2019; Chen et al. 2020), see also Chen (2024), Li et al. (2024), and Chen et al. (2024). But the estimation of the efficient price volatility matrix has been overlooked in the presence of staleness. This oversight could introduce bias in the volatility matrix estimation when staleness is high. This is a second motivation of the present paper.

This article estimates spot systematic and idiosyncratic volatility of the efficient price processes using local factor analysis as well as their integrated versions by aggregating the non-overlapping local volatility proxies. We observe that while the estimated covolatilities are biased, the volatility estimates remain unbiased. We also derived the concentration-type inequalities for spot volatility matrix and its inverse. After locally correcting the bias due to the price staleness, we obtain a consistent and unbiased estimator. It is interesting to preview two results: 1) the staleness correction worsens the convergence rates of the volatility estimates in a factor of dimension  $d$ ; more precisely, the staleness-corrected estimates of the systematic covolatilities (spot or integrated) have lower convergence rate ( $d^{-1/2}$  in  $d$ ) than the uncorrected ( $d^{-1}$  in  $d$ ); nevertheless, the bias-corrected estimates are consistent, and our empirical studies demonstrate that the staleness correction leads to reduced out-of-sample portfolio risk almost uniformly in tested gross exposure levels; 2) the factors in the sample size  $n$  of the convergence rates of the integrated estimates are much smaller than those of the spot estimates, validating the aggregation efficiency after nonlinear factor analysis.

The rest of this article is organized as follows. Section 2 introduces the SFM, presenting the model estimation procedure and key theoretical results. Section 3 outlines the estimation procedure for effective price volatility matrices along with the corresponding theoretical results. Section 4 offers a simulation study evaluating finite-sample performance. Section 5 contains our empirical analysis. Section 6 concludes. All proofs and supplementary results are provided in the Supplementary Appendix.

To end this section, we introduce some notations that are used throughout the paper. We use  $\|A\|$  to represent the spectral norm of a matrix  $A$  or the Euclidean norm of a vector  $A$ . The Frobenius norm of a matrix  $A$  is denoted by  $\|A\|_F$ . The  $L_1$  norm of a matrix  $A$  is defined as  $\max_j \sum_i |A_{ij}|$  and the weighted quadratic norm  $\|A\|_\Sigma$  is  $d^{-1/2} \|\Sigma^{-1/2} A \Sigma^{-1/2}\|_F$ . Let  $a \wedge b = \min\{a, b\}$  and  $a \vee b = \max\{a, b\}$ .  $\mathbf{1}_d$  is a vector that all elements are 1.  $r_{\min}(A)$  and  $r_{\max}(A)$  are the minimum and maximum eigenvalues of  $A$ , respectively, ordered in  $\lambda_{\max}(A) = \lambda_1(A) \geq \lambda_2(A) \geq \dots \geq \lambda_{\min}(A)$ .  $C$  is a generic positive constant that may vary from line to line.  $I_r$  is an  $r$ -dimensional identity matrix. The operator  $\circ$  represents Hadamard product and  $\otimes$  stands for Kronecker product. We use  $\xrightarrow{P}$ ,  $\mathcal{L}|\mathcal{F}$ , and  $\mathcal{L}_s|\mathcal{F}$  to denote convergence in probability,  $\mathcal{F}$ -conditional convergence in law (i.e., weak convergence), and  $\mathcal{F}$ -conditional stable convergence in law, respectively. For any function  $f$ ,  $f^{(i)}$  is the  $i$ th order derivative of  $f$ . We specify the structure of the  $\sigma$ -field  $\mathcal{F}$ . We have the following flows of information on  $\mathcal{F}$ : 1)  $(\mathcal{F}_t^{(p)})_{t \geq 0}$  is the natural filtration associated with the staleness probability process; 2)  $\mathcal{F}_{t_j, n}^{(b)}$  is the  $\sigma$ -algebra generated by the random variables  $b_{t_0, n}, b_{t_1, n}, \dots, b_{t_j, n}$ , which is a discrete filtration associated with a partition of the fixed time interval  $[0, T]$ ; and 3)  $(\mathcal{F}_t)_{t \geq 0}$  is the natural filtration associated with the efficient price process. Moreover, we write  $\mathcal{F}_\infty = \vee_{t > 0} \mathcal{F}_t$ .

## 2 Price Staleness Factor Analysis

### 2.1 Price Staleness Factor Model

We observe a large intra-day panel of asset log-prices,  $\tilde{Y}$  at discrete times  $t_0, t_1, \dots, t_n$  over a finite time interval  $[0, T]$ , where  $t_j = j\Delta_n$  with  $\Delta_n$  being the sampling frequency and  $n = \lfloor T/\Delta_n \rfloor$ . The effective price  $Y$  is partially observable and it depends on if price staleness occurs or not. Extending the model (1) to the  $d$ -dimensional case,  $\tilde{Y}$  can be expressed as follows.<sup>1</sup>

$$\tilde{Y}_{t_j} = Y_{t_j} \circ (\mathbf{1}_d - B_{t_j}) + \tilde{Y}_{t_{j-1}} \circ B_{t_j}, \quad (2)$$

where  $B_{t_j} = (B_{1t_j}, \dots, B_{dt_j})'$  is a  $d$ -dimensional vector of binary (Bernoulli) variables, the efficient log price  $\{Y_t, t \geq 0\}$  is a  $d$ -dimensional continuous-time Itô-semimartingale. When  $B_{it_j} = 1$ , implying that zero occurs,  $\tilde{Y}_{it_j}$  is the lagged value  $\tilde{Y}_{it_{j-1}}$ , and otherwise  $\tilde{Y}_{it_j}$  is the

<sup>1</sup>There are two possible causes of zeros (zero returns): the absorption of limited trading volume without price impact (defined as excess staleness) and price discretization (price rounding). The implicit differences between these two are discussed in [Bandi et al. \(2020\)](#).

efficient price  $Y_{it_j}$ .

In most previous studies in the high-frequency data analysis literature often ignored the existence of price staleness, i.e.,  $B = 0$  is assumed typically, c.f., [Mykland and Zhang \(2009\)](#), [Chen et al. \(2020\)](#), and [Chen et al. \(2024\)](#). Ever since [Bandi et al. \(2017\)](#), price staleness began to be considered formally. [Bandi et al. \(2024\)](#) was the first to examine price staleness using high-dimensional data, employing a two-layer Bernoulli variable structure to study systematic staleness. To tackle with the limitations mentioned in the introduction, we develop a new and flexible model for studying systematic and idiosyncratic staleness in high dimension.

We rewrite the Bernoulli random variable  $B_{it}$  as  $B_{it} = \mathbb{1}_{\{b_{it} \leq p_{it}\}}$ , where  $\mathbb{1}_{\{\cdot\}}$  is the indicator function and  $\{b_{it}\}_{t \in [0, T]}$  is a collection of uniformly distributed random variables. Given the information set  $\mathcal{F}^{(p)}$ , the Bernoulli random variables  $B_{it}$  and  $B_{ms}$  are independent  $\forall t \neq s$  or  $i \neq m$ . The mutual independence of the  $B_{it}$ 's implies that the duration, defined as the time between price updates, converges in probability to zero as  $n \rightarrow \infty$ . In addition,  $p_t = (p_{1t}, \dots, p_{dt})'$  is modeled as a continuous-time stochastic process to capture how likely the zeros occur, which is independent of the efficient price and its volatility. Inspired by the generalized linear model, we define  $p_{it} = \Psi(z_{it})$ , where  $\Psi: \mathbb{R} \rightarrow (0, 1)$  is an increasing function in  $\mathcal{C}^3$ . The process  $z_{it}$  is modeled as a Itô semimartingale, defined as follows:

$$z_{it} = a_i' x_{it} + \gamma_i' g_t, \quad i = 1, \dots, d,$$

where  $x_{it}$  is an  $r_x$  dimensional stochastic process (covariate),  $a_i$  is the coefficient vector,  $g_t$  is an  $r_g$  dimensional continuous-time factor process independent of  $x_t = (x_{1t}, \dots, x_{dt})$ , and  $\gamma_i$  is a vector of factor loadings describing the exposure to the systematic factors. The covariate  $x_i$  for the  $i$ th asset could be the trading volume and liquidity.

Next, we assume the processes  $x_i$  and  $g$  are locally bounded Itô semimartingales,

$$x_{it} = x_{i0} + \int_0^t \mu_{is}^x ds + \int_0^t \sigma_{is}^x dW_{is}^x, \quad g_t = g_0 + \int_0^t \mu_s^g ds + \int_0^t \sigma_s^g dW_s^g,$$

where  $W_i^x$  and  $W^g$  are  $r_x$ -dimensional and  $r_g$ -dimensional Brownian motions, respectively. The coefficients  $\mu_i^x$  and  $\mu^g$  are progressively measurable, and  $\sigma_i^x$  and  $\sigma^g$  are adapted càdlàg processes. Notably, we only observe the stochastic process  $x_i$  and the Bernoulli random variables  $B_i$ , but not  $p_{it}$  or  $z_{it}$ . This poses a challenge that the GPCA in [Ait-Sahalia and Xiu \(2017\)](#) and [Pelger \(2019\)](#) and the LPCA in [Kong \(2017, 2018\)](#); [Kong et al. \(2023\)](#) are not applicable any more, because the differential form of  $z_{it}$  (or  $p_{it}$ ) is no longer observable at discrete time instances. A

new method that can handle the nonstationary integral form of  $z_{it}$  with continuous-time factor structure has to be invented. While it would be interesting to consider jumps in these processes, this article does not include them in  $x_{it}$  and  $g_t$  due to the added complexity they introduce in our proposed MLE.<sup>2</sup> The consideration of jumps is left for future work.

Before giving the maximum likelihood estimation method for a latent nonlinear nonstationary factor model, we give some regularity assumptions on the staleness factor model.

**Assumption 1.** 1.  $\|d^{-1}\Gamma\Gamma' - I_{r_g}\| \rightarrow 0$  where  $\Gamma = (\gamma_1, \dots, \gamma_d)'$ .  $\max_{1 \leq i \leq d} \|\gamma_i\|_F \leq C$ . There exists a locally bounded process  $C_t$  such that  $\sup_{t \in [0, T]} \|x_{i,t}\|_F \leq C_t$  and  $\sup_{t \in [0, T]} \|g_t\|_F \leq C_t$  for all  $i = 1, \dots, d$ .

2. There exist constant  $\bar{p}$  ( $0 < \bar{p} < 1$ ) such that  $\sup_{t \in [0, T]} \max_{1 \leq i \leq d} p_{it} \leq \bar{p}$ . Moreover, we have  $\inf_{t \in [0, T]} \min_{1 \leq i \leq d} p_{it} > 0$ . We define  $\Xi = \{p : 0 < p \leq \bar{p}\}$ .

3.  $|\psi^{(j)}(z)| < C$  for any  $z \in \Xi$ , where  $\psi(z) := \frac{d\Psi(z)}{dz}$  and  $\Xi = \{z : 0 < \Psi(z) \leq \bar{p}\}$ .

Assumption 1.1 is standard in high-frequency factor analysis, c.f., [Ait-Sahalia and Xiu \(2017\)](#) and [Kong \(2017, 2018\)](#). Assumption 1.2 is mild and appeared in [Bandi et al. \(2023\)](#). Assumption 1.3 is primarily to ensure that the derivative of the log-likelihood function (defined in Section 2.2) is bounded.

The following notations are related to the asymptotic variances. Let

$$\Omega_u = \text{diag}\{\Omega_{u,1}, \dots, \omega_{u,d}\}, \quad \Omega_\gamma = \text{diag}\{\Omega_{\gamma,1}, \dots, \omega_{\gamma,n+1}\}, \quad \Omega_{u\gamma} = \{\Omega_{u\gamma,ij}\}_{d(r_x+r_g) \times (n+1)r_g},$$

where

$$\Omega_{u,i} = \frac{1}{T} \int_0^T \frac{\psi^2(z_{it})}{\Psi(z_{it})(1-\Psi(z_{it}))} u_{it} u'_{it} dt, \quad \Omega_{\gamma,j} = \text{plim}_{d \rightarrow \infty} \frac{1}{d} \sum_{i=1}^d \frac{\psi^2(z_{it_j})}{\Psi(z_{it_j})(1-\Psi(z_{it_j}))} \gamma_i \gamma'_i,$$

$$\Omega_{u\gamma,ij} = \frac{\psi^2(z_{it_j})}{\Psi(z_{it_j})(1-\Psi(z_{it_j}))} u_{it_j} \gamma'_i.$$

**Assumption 2.** 1.  $\Omega_{u,i}$  and  $\Omega_{\gamma,j}$  are positive definite for  $1 \leq i \leq d$  and  $0 \leq j \leq n$ .  $r_{\max}(\Omega_u)$ ,  $r_{\max}(\Omega_\gamma)$ ,  $r_{\max}(\Omega_u^{-1})$ ,  $r_{\max}(\Omega_\gamma^{-1})$ ,  $\frac{1}{nd} \Omega'_{u\gamma} \Omega_u^{-1} \Omega_{u\gamma}$  and  $\frac{1}{nd} \Omega_{u\gamma} \Omega_\gamma^{-1} \Omega'_{u\gamma}$  are all finite.

2.  $\max_{t \in [0, T]} \left\| \frac{1}{d} \sum_{i=1}^d \frac{\psi^2(z_{it})}{(1-\Psi(z_{it}))\Psi(z_{it})} \gamma_i \gamma'_i - \Omega_{\gamma t}^* \right\|_F = o_P(1)$  as  $d \rightarrow \infty$ , where  $\Omega_{\gamma t}^* = \text{plim}_{d \rightarrow \infty} \frac{1}{d} \sum_{i=1}^d \frac{\psi^2(z_{it})}{(1-\Psi(z_{it}))\Psi(z_{it})} \gamma_i \gamma'_i$ .

---

<sup>2</sup>In our binary observables, the usual techniques for dealing with jumps are no longer applicable, e.g., [Mancini \(2009\)](#).



Assumption 2.1 is used for deriving the inverse of the Hessian matrix. Similar assumptions appeared in Gao et al. (2023) for low-frequency panel data. Assumption 2.2 is made to ensure that the asymptotic variance of the cross section is uniformly convergent. We emphasize that the converging asymptotic variance is guaranteed by the in-fill theory.

## 2.2 Estimation of the Staleness Factor Model

Unlike traditional long span ( $T \rightarrow \infty$ ) nonlinear factor models, the SFM is inherently non-stationary within any fixed time window  $[0, T]$  which is typical in high-frequency data analysis. As a result, many of the well established methodologies in large-dimensional factor analysis are not directly applicable to our nonstationary framework. One would think of using PCA (Ait-Sahalia and Xiu 2017; Pelger 2019) or LPCA (Kong et al. 2023) on the high-frequency increments of  $z_t = (z_{1t}, \dots, z_{dt})'$ , but  $z_t$  itself is not observable making the differential form unavailable. To estimate the SFM, we employ a nonstationary MLE. Define the increments of the observed covariate  $x$  and latent factor  $g$  by

$$\Delta x_{it_j} := x_{it_j} - x_{it_{j-1}} \quad \text{and} \quad \Delta g_{t_j} := g_{t_j} - g_{t_{j-1}},$$

for  $j = 1, \dots, n$ . We use the convention that  $\Delta x_{it_0} := x_{it_0}$  and  $\Delta g_{t_0} := g_{t_0}$ . We next rewrite  $z_{it}$  in the integrated form of diminishing increments:

$$z_{it_j} = a'_i \sum_{l=0}^j \Delta x_{it_l} + \gamma'_i \sum_{l=0}^j \Delta g_{t_l}.$$

Since  $z_{it_j}$  is latent, unlike returns data, we cannot estimate  $\Delta g_{t_j}$  by directly analyzing  $\Delta z_{it_j}$ . Instead, we can only use the aggregated form  $z_{it_j}$ . Let

$$A = (a_1, \dots, a_d)', \quad \Gamma = (\gamma_1, \dots, \gamma_d)', \quad G = (g_{t_0}, g_{t_1}, \dots, g_{t_n})', \quad \Delta G = (\Delta g_{t_0}, \dots, \Delta g_{t_n})',$$

and  $\theta_i = (a'_i, \gamma'_i)'$ ,  $\Theta = (A, \Gamma)$ ,  $u_{it} = (x'_{it}, g'_i)'$ . The relationship between  $G$  and  $\Delta G$  is  $G = (\varrho \otimes I_{r_g}) \Delta G$ , where  $\varrho = (\mathbf{1}_{\{i \leq j\}})_{i=1, \dots, n+1}^{j=1, \dots, n+1}$  is a  $(n+1) \times (n+1)$  dimensional matrix with the lower triangular and diagonal entries being 1 and others 0.

A well known fact of the factor model is that  $\gamma_i$  and  $\Delta g_{t_j}$  (or  $g_{t_j}$ ) cannot be separately identified without imposing normalization. We choose the following normalization in the SFM:

$$\Gamma \in \mathcal{G} = \left\{ \Gamma \mid \frac{\Gamma' \Gamma}{d} = I_{r_g} \right\}, \quad \Delta G \in \mathcal{G} := \left\{ \Delta G \mid \frac{\Delta G' \Delta G}{n+1} \text{ is diagonal with distinct values} \right\}. \quad (3)$$

Now, the  $\mathcal{F}^{(p)}$ -conditional likelihood function is

$$L(A, \Gamma, \Delta G) := \prod_{i=1}^d \prod_{j=0}^n \left[ 1 - \Psi \left( a'_i x_{it_j} + \gamma'_i \sum_{l=0}^j \Delta g_{t_l} \right) \right]^{1-B_{it_j}} \Psi \left( a'_i x_{it_j} + \gamma'_i \sum_{l=0}^j \Delta g_{t_l} \right)^{B_{it_j}},$$

and its log-scale form is ( recall  $z_{it_j} = a'_i x_{it_j} + \gamma'_i \sum_{l=0}^j \Delta g_{t_l}$ )

$$\mathbb{L}_{d,n}(A, \Gamma, \Delta G) := \sum_{i=1}^d \sum_{j=0}^n \left\{ (1 - B_{it_j}) \log [1 - \Psi(z_{it_j})] + B_{it_j} \log \Psi(z_{it_j}) \right\}.$$

Then the MLE of  $\{\hat{A}, \hat{\Gamma}, \hat{\Delta G}\}$  is given by

$$(\hat{A}, \hat{\Gamma}, \hat{\Delta G}) = \arg \max_{A \in \mathbb{R}^{d \times r_x}, \Gamma \in \mathcal{G}, \Delta G \in \mathcal{G}} \mathbb{L}_{d,n}(A, \Gamma, \Delta G). \quad (4)$$

It can be easily seen that, unlike the high-frequency PCA (Global or Local) our estimator does not have analytical closed form. This makes it difficult in the derivation of the large sample property and computation. It turns out, as demonstrated by Theorem 1, the MLE achieves the same convergence rate as the high-frequency PCA estimation. We first give the computational algorithm. Let  $l_{i,j}(z_{it_j}) = \left\{ (1 - B_{it_j}) \log [1 - \Psi(z_{it_j})] + B_{it_j} \log \Psi(z_{it_j}) \right\}$ , and define

$$\mathbb{L}_{i,n}(\theta_i, \Delta g) = \sum_{j=0}^n l_{i,j}(z_{it_j}), \quad \mathbb{L}_{d,j}(\theta, \Delta g_{t_j}) = \sum_{i=1}^d \sum_{l=j}^n l_{i,l}(z_{it_l}).$$

Note that  $\mathbb{L}_{d,n}(A, \Gamma, \Delta G) = d^{-1} \sum_{i=1}^d \mathbb{L}_{i,n}(\theta_i, \Delta g)$ .

We now propose the following iterative procedure:

Step 1: Choose the initial values of  $\Delta G^{(0)}$  and  $\Theta^{(0)}$ .

Step 2: Given  $\Delta G^{(l-1)}$ , solve  $\theta_i^{(l-1)} = \arg \max_{\theta} \mathbb{L}_{i,n}(\theta, \Delta g^{(l-1)})$  for  $i = 1, \dots, d$ ; given  $\Theta^{(l-1)}$ , solve  $\Delta g_{t_j}^{(l)} = \arg \max_{\Delta g} \mathbb{L}_{d,j}(\theta, \Delta g^{(l-1)})$  for  $j = 0, 1, \dots, n$ .

Step 3: Repeat the second step until  $\mathbb{L}_{d,n}(A^{(l^*)}, \Gamma^{(l^*)}, \Delta G^{(l^*)})$  is sufficiently close to  $\mathbb{L}_{d,n}(A^{(l^*)}, \Gamma^{(l^*)}, \Delta G^{(l^*-1)})$ , for  $l = 1, \dots, l^*$ .

Step 4: Normalize  $\Gamma^{(l^*)}$  and  $\Delta G^{(l^*)}$  so that they satisfy the normalization in (3); set  $G$  by  $G^{(l^*)} = (\varrho \otimes I_{r_g}) \Delta G^{(l^*)}$ .

In Step 1, we use a local block approach to estimate the staleness probability  $p_{it_j}$  (similar to the method referenced in Kong 2017, 2018). We then apply the inverse map to obtain  $z_{it_j} = \Psi^{-1}(p_{it_j})$  and regress  $z_{it_j}$  against  $x_{it_j}$  for  $j = 0, \dots, n$  to get the estimate  $\tilde{a}_i$ . Next, we

compute the residual  $z_{it_j} - \tilde{a}'_i x_{it_j}$ , for which we use the high-frequency PCA based on [Pelger \(2019\)](#) to estimate  $\Gamma$  and  $\Delta G$ . These are used as the initial estimates. In Step 3, we set the tolerance condition as:

$$\frac{1}{d} \sum_{i=1}^d \|a_i^{(l^*)} - a_i^{(l^*-1)}\|_F^2 + \frac{1}{nd} \|G^{(l^*)} \Gamma^{(l^*)} - G^{(l^*-1)} \Gamma^{(l^*-1)}\|_F^2 < \varepsilon,$$

for sufficiently small  $\varepsilon > 0$ , e.g.,  $10^{-3}$ . In step 4, performing the diagonalisation to obtain

$$\left( \frac{1}{d} \Gamma^{(l^*)'} \Gamma^{(l^*)} \right)^{1/2} \left( \frac{1}{n+1} \Delta G^{(l^*)'} \Delta G^{(l^*)} \right) \left( \frac{1}{d} \Gamma^{(l^*)'} \Gamma^{(l^*)} \right)^{1/2} = \Gamma \Psi \Gamma',$$

where  $\Gamma$  is an orthogonal matrix and  $\Psi$  is a diagonal matrix. The final numerical solutions for  $\Gamma$  and  $\Delta G$  are  $\Gamma^{(l^*)} \left( \frac{1}{d} \Gamma^{(l^*)'} \Gamma^{(l^*)} \right)^{-1/2} \Gamma$  and  $\Delta G^{(l^*)} \left( \frac{1}{d} \Gamma^{(l^*)'} \Gamma^{(l^*)} \right)^{1/2} \Gamma$ , respectively.

To consistently determine the number of factors, we use the method proposed by [Pelger 2019](#), which examines the ratio of adjacent eigenvalues. Specifically, let the ordered eigenvalues of  $(\hat{\Gamma} \Delta \hat{G}') (\hat{\Gamma} \Delta \hat{G}')'$  be  $\tilde{\lambda}_1 \geq \dots \geq \tilde{\lambda}_{r_g^{\max}}$  where  $r_g^{\max}$  is a prespecified large constant. The perturbed eigenvalues are defined as  $\hat{\lambda}_k = \tilde{\lambda}_k + \xi_{nd}$  where  $\xi_{nd}$  is the median eigenvalue rescaled by  $\sqrt{d}$ . The perturbation term  $\xi_{nd}$  is any slowly increasing sequence such that  $\xi_{nd}/d \rightarrow 0$  and  $\xi_{nd} \rightarrow \infty$ . The estimated number of factors is estimated by

$$\hat{r}_g(\chi) = \max\{k \leq r_g^{\max} - 1 : ER_k > 1 + \chi\}, \quad \chi > 0,$$

where  $ER_k = \hat{\lambda}_k / \hat{\lambda}_{k+1}$ .

### 2.3 Results for Staleness Factor Analysis

It is worth noting that  $\Delta g_{t_j}$  tends to 0 as  $\Delta_n$  tends to 0 ( $T$  fixed and  $n \rightarrow \infty$ ). We might also estimate the properly normalized factor increments, but the asymptotic statements will be formulated on evaluating the stochastic process  $g$  at a discrete time point  $t_j$ , i.e.,  $g_{t_j} = \sum_{k=0}^j \Delta g_{t_k}$ . Let  $\omega_{nd} = \min(\sqrt{n}, \sqrt{d})$ . The following proposition provides the convergence of  $\hat{\theta}_i$  and  $\hat{g}_{t_j}$ .

**Proposition 1.** (*Consistency*). *Assuming that Assumptions 1 and 2 hold, we posit the existence of a constant  $\delta^\dagger$  such that  $\frac{d}{n^{1+\delta^\dagger}} = o(1)$ .*

$$(i) \quad \frac{1}{\sqrt{d}} \|\hat{\Theta} - \Theta\|_F = O_P(\omega_{nd}^{-1}), \quad \|\hat{g}_{t_j} - g_{t_j}\| = O_P(\omega_{nd}^{-1}), \quad \text{and} \quad |\hat{\gamma}'_i \hat{g}_{t_j} - \gamma'_i g_{t_j}| = O_P(\omega_{nd}^{-1}).$$

$$(ii) \quad \text{As } \omega_{n,d} \rightarrow \infty,$$

$$\sum_{j=1}^n (\hat{a}'_i \Delta x_{it_j})(\hat{a}'_m \Delta x_{mt_j}) = a'_i[x_i, x_m]_T a_m + O_P(n^{-1/2}),$$

and if  $n/d \rightarrow 0$ ,

$$\sum_{j=1}^n \Delta \hat{g}_{t_j} \Delta \hat{g}'_{t_j} = [g, g]_T + o_P(1), \quad \sum_{j=1}^n (\hat{\gamma}'_i \Delta \hat{g}_{t_j})(\hat{\gamma}'_m \Delta \hat{g}_{t_j}) = \gamma'_i [g, g]_T \gamma_m + o_P(1).$$

Proposition 1 provides the convergence for the quadratic variation of the estimators. However, estimating the factor component requires stricter conditions, as both the factors and their loadings must be estimated, whereas covariate estimation involves only the coefficients.

We now demonstrate that the estimators for the factor loadings and factors converge stably in law to mixed Gaussian distributions.<sup>3</sup>

**Proposition 2.** (*Asymptotic Distribution of Loadings and Factors*). *Under the conditions in Proposition 1, as  $\omega_{n,d} \rightarrow \infty$ .*

(i) If  $\frac{\sqrt{n}}{d} \rightarrow 0$ ,

$$n^{1/2} (\hat{\theta}_i - \theta_i) \xrightarrow{\mathcal{L}_s | \mathcal{F}^{(p)}} \mathcal{N}(0, \Omega_{u,i}^{-1}),$$

$$\text{where } \Omega_{u,i} = \frac{1}{T} \int_0^T \frac{\psi^2(z_{it})}{\Psi(z_{it})(1-\Psi(z_{it}))} u_{it} u'_{it} dt.$$

(ii) If  $\frac{\sqrt{d}}{n} \rightarrow 0$ ,

$$d^{1/2} (\hat{g}_{t_j} - g_{t_j}) \xrightarrow{\mathcal{L} | \mathcal{F}^{(p)}} \mathcal{N}(0, \Omega_{\gamma,j}^{-1}),$$

$$\text{where } \Omega_{\gamma,j} = \text{plim}_{d \rightarrow \infty} \frac{1}{d} \sum_{i=1}^d \frac{\psi^2(z_{it_j})}{\Psi(z_{it_j})(1-\Psi(z_{it_j}))} \gamma_i \gamma'_i.$$

Note that the mode of convergence is stable convergence in law. The asymptotic distribution of  $\hat{\theta}_i$  is mainly determined by the serial partial sums of the weighted Bernoulli variates, and the asymptotic distribution of  $\hat{g}_{t_j}$  is determined by the cross-sectional partial sums of the weighted Bernoulli variates. Note that we study the asymptotic distribution of the cumulative sum of the increments, i.e., the factor processes evaluated at some terminal time.

Based on Propositions 1 and 2, we establish the consistency and asymptotic normality for the estimated  $p_{it_j}$ .

---

<sup>3</sup>The classical results on stable convergence proposed by Hall and Heyde (2014) do not hold under the filtration  $\mathcal{F}_{t_n, n}^{(b)}$ , as the condition of nested filtrations is no longer satisfied. Nonetheless, this issue can be addressed using Theorem 1 and Corollary 3 from Kolokolov et al. (2020).

**Theorem 1.** (Statistical Properties of  $p_{it_j}$ ). Assuming that Assumptions 1 and 2 hold, we posit the existence of a constant  $\delta^\dagger$  such that  $\frac{d}{n^{1+\delta^\dagger}} = o(1)$ .

(i)  $\hat{p}_{it_j} - p_{it_j} = O_P(\omega_{nd}^{-1})$  for  $i = 1, \dots, d$ .

(ii)  $\omega_{nd}(\hat{p}_{it_j} - p_{it_j}) \xrightarrow{\mathcal{L}|\mathcal{F}^{(p)}} \mathcal{N}_1$ , where  $\mathcal{N}_1$  is defined on an extension of the probability space, and conditionally on  $\mathcal{F}^{(p)}$  is centered Gaussian with (conditional) variance

$$\Omega_{it_j}^{(p)} = \psi^2(z_{it_j}) \left( \frac{\omega_{nd}^2}{n} u'_{it_j} \Omega_{u,i}^{-1} u_{it_j} + \frac{\omega_{nd}^2}{d} \gamma'_i \Omega_{\gamma,j}^{-1} \gamma_i \right). \quad (5)$$

The statistical properties of  $\hat{p}_{it_j}$  rely on the  $i$ th serial partial sums and  $j$ th cross-sectional partial sums of the Bernoulli variates. The mode of convergence here is stable convergence in law, which is a stronger notion compared to convergence in distribution. The theorem delineated in Theorem 1 (ii) manifests two notable special cases: 1) when the ratio  $d/n \rightarrow 0$ ,  $\sqrt{d}(\hat{p}_{it_j} - p_{it_j}) \xrightarrow{\mathcal{L}|\mathcal{F}^{(p)}} \mathcal{N}\left(0, \psi^2(z_{it_j}) \gamma'_i \Omega_{\gamma,j}^{-1} \gamma_i\right)$ ; 2) otherwise,  $\sqrt{n}(\hat{p}_{it_j} - p_{it_j}) \xrightarrow{\mathcal{L}|\mathcal{F}^{(p)}} \mathcal{N}\left(0, \psi^2(z_{it_j}) u'_{it_j} \Omega_{u,i}^{-1} u_{it_j}\right)$ . These results underscore the nuanced behavior of our model under different conditions, shedding light on its statistical properties under contrasted scenarios.

To make the CLT feasible, one needs consistent estimator  $\hat{\Omega}_{it_j}^{(p)}$  of the conditional variance  $\Omega_{it_j}^{(p)}$  in (5). In view of Proposition 1 and Theorem 1 (i), this is easily accomplished by defining

$$\begin{aligned} \hat{\Omega}_{it_j}^{(p)} = & \psi^2(\hat{z}_{it_j}) \left[ \frac{\omega_{nd}^2}{n} \hat{u}'_{it_j} \left( \frac{1}{n} \sum_{j=0}^n \frac{\psi^2(\hat{z}_{it_j})}{\Psi(\hat{z}_{it_j})(1 - \Psi(\hat{z}_{it_j}))} \hat{u}_{it_j} \hat{u}'_{it_j} \right)^{-1} \hat{u}_{it_j} \right. \\ & \left. + \frac{\omega_{nd}^2}{d} \hat{\gamma}'_i \left( \frac{1}{d} \sum_{i=1}^d \frac{\psi^2(\hat{z}_{it_j})}{\Psi(\hat{z}_{it_j})(1 - \Psi(\hat{z}_{it_j}))} \hat{\gamma}_i \hat{\gamma}'_i \right)^{-1} \hat{\gamma}_i \right], \end{aligned}$$

where  $\hat{u}_{it_j} = (x'_{it_j}, \hat{g}_{it_j})'$ . By the mode of stable convergence and since  $\Omega_{it_j}^{(p)}$  is  $\mathcal{F}_\infty^{(p)}$  measurable, we soon have the following corollary.

**Corollary 1.** Under the conditions in Theorem 1,

$$\frac{\omega_{nd}}{\sqrt{\hat{\Omega}_{it_j}^{(p)}}} (\hat{p}_{it_j} - p_{it_j}) \xrightarrow{\mathcal{L}|\mathcal{F}^{(p)}} \mathcal{N}(0, 1),$$

where  $\mathcal{N}(0, 1)$  is a standard normal random variable and independent of  $\mathcal{F}^{(p)}$ .

Besides the pointwise convergence in the time window as shown in Theorem 1 and Corollary 1, we next introduce a global convergence result of the estimated processes in the whole time

window. The integral functional of two staleness probability processes is useful (see Theorem 5). Define a function  $\phi: (0, 1)^2 \rightarrow \mathbb{R}$  to be locally bounded and in  $\mathcal{C}^2$ , we are interested in the following integral functional:

$$U_{im}(\phi) = \int_0^T \phi(p_{it}, p_{mt}) dt \text{ for } i \neq m.$$

A natural estimator is through Riemann sum approximation and plug-in principal, which is defined as

$$U_{im}^n(\Delta_n, \phi) = \Delta_n \sum_{j=0}^n \phi(\hat{p}_{it_j}, \hat{p}_{mt_j}).$$

The following theorem gives the consistency and asymptotic normality of the functional estimator.

**Theorem 2.** (*Statistical Properties of the integrated functional*). *Assuming that Assumptions 1 and 2 hold, we posit the existence of a constant  $\delta^\dagger$  such that  $\frac{d}{n^{1+\delta^\dagger}} = o(1)$ . Let  $\phi: \Xi^2 \rightarrow \mathbb{R}$  be a locally bounded  $\mathcal{C}^2$  function such that  $|\partial^{j,k} \phi(x, y)| \leq C(1 + |x|^{q'-j} + |y|^{q'-k})$  for  $j, k = 0, 1, 2$  and  $q' \geq 2$ . As  $d \wedge n \rightarrow \infty$ ,*

$$(i) U_{im}^n(\Delta_n, \phi) \xrightarrow{P} \int_0^T \phi(p_{it}, p_{mt}) dt.$$

$$(ii) \Delta_n^{-1/2} (U_{im}^n(\Delta_n, \phi) - U_{im}(\phi)) \xrightarrow{\mathcal{L}_s | \mathcal{F}_\infty^{(p)}} \frac{1}{\sqrt{T}} \left( \int_0^T \partial_1 \phi(p_{it}, p_{mt}) u'_{it} dt \right) \Omega_{u,i}^{-1} \mathcal{N}_2 \\ + \frac{1}{\sqrt{T}} \left( \int_0^T \partial_2 \phi(p_{it}, p_{mt}) u'_{mt} dt \right) \Omega_{u,m}^{-1} \mathcal{N}_3,$$

where  $\mathcal{N}_2$  and  $\mathcal{N}_3$  are defined on an extension of the original probability space,  $\partial_1 \phi(x, y) = \frac{\partial \phi(x, y)}{\partial x}$  and  $\partial_2 \phi(x, y) = \frac{\partial \phi(x, y)}{\partial y}$ . Conditionally on  $\mathcal{F}^{(p)}$ ,  $\mathcal{N}_2$  and  $\mathcal{N}_3$  are independent centered Gaussian variables with covariance matrices  $\Omega_{u,i}$  and  $\Omega_{u,m}$ , respectively.

To make this CLT feasible in inference, we provide the plug-in version of the limiting variance in Theorem 2 (ii). See the following corollary.

**Corollary 2.** *Under the conditions in Theorem 2,*

$$\Delta_n^{-1/2} \frac{(U_{im}^n(\Delta_n, \phi) - U_{im}(\phi))}{\sqrt{\tilde{\Omega}_{u,i} + \tilde{\Omega}_{u,m}}} \xrightarrow{\mathcal{L}_s | \mathcal{F}_\infty^{(p)}} \mathcal{N}(0, 1),$$

where  $(\tilde{\Omega}_{u,m})$  is similarly defined)

$$\tilde{\Omega}_{u,i} = \frac{\Delta_n}{\sqrt{T}} \sum_{j=0}^n \partial_1 \phi(\hat{p}_{it_j}, \hat{p}_{mt_j}) \hat{u}'_{it_j} \left( \sum_{j=0}^n \frac{\psi^2(\hat{z}_{it_j})}{\Psi(\hat{z}_{it_j})(1 - \Psi(\hat{z}_{it_j}))} \hat{u}_{it_j} \hat{u}'_{it_j} \right)^{-1} \sum_{j=0}^n \partial_1 \phi(\hat{p}_{it_j}, \hat{p}_{mt_j}) \hat{u}_{it_j}.$$

**Remark 1.** An important equation for deriving Theorem 2 is (see the Supplementary Material)

$$\hat{p}_{it_j} - p_{it_j} = \psi(z_{it_j}) u'_{it_j} \Omega_{u,i}^{-1} \frac{1}{n} \sum_{k=0}^n \varepsilon_{it_k} \psi(z_{it_k}) u_{it_k} + \psi(z_{it_j}) \gamma'_i \Omega_{\gamma,j}^{-1} \frac{1}{d} \sum_{m=1}^d \varepsilon_{mt_j} \psi(z_{mt_j}) \gamma_m + o_P(\omega_{nd}^{-1}),$$

where  $\varepsilon_{it_j} = \frac{B_{ij} - \Psi(z_{it_j})}{(1 - \Psi(z_{it_j})) \Psi(z_{it_j})}$ . We note that the result related to the  $\sum_{m=1}^d \varepsilon_{mt_j} \psi(z_{mt_j}) \gamma_m$  does not appear in Theorem 2.

The two dominant terms in Remark 1 are caused by  $\hat{\theta}_i$  and  $\hat{g}_{t_j}$ , respectively, and are  $\mathcal{F}^{(p)}$ -conditionally asymptotically independent of each other.

**Remark 2.** Estimating  $U_{im}(\phi)$  typically follows the estimation of  $p_t$ . Unlike [Kolokolov et al. \(2020\)](#) who used the local block method, we employ MLE. Estimating functionals of interest via the local block method can introduce errors, such as edge effects and nonlinear bias (see [Jacod and Rosenbaum 2013](#); [Jacod and Todorov 2014](#); [Li et al. 2019](#)). These errors are influenced by the window size in the local block method, whereas our MLE-based estimator avoids these issues, benefiting from the inherent nature of maximum likelihood estimation.

### 3 Efficient Price Volatility Estimation

#### 3.1 Efficient Price Process

We assume the efficient price process  $Y$ , defined on a filtered probability space  $(\Omega, \mathcal{F}, \{\mathcal{F}_t\}_{t \geq 0}, \mathbb{P})$ , takes the following form with continuous-time factor structure:

$$Y_{it} = Y_{i0} + \int_0^t \mu_{is} ds + \sum_{l=1}^r \int_0^t \sigma_{is}^l dW_s^l + \int_0^t \sigma_{is}^* dW_{is}^*, \quad 1 \leq i \leq d, \quad (6)$$

where  $\mu_i$ 's,  $\sigma_i^l$ 's ( $1 \leq l \leq r$ ),  $\sigma_i^*$ 's are locally bounded adapted processes and  $W = (W^1, \dots, W^r)'$  is an  $r$ -dimensional standard Brownian motion and  $W^* = (W_1^*, \dots, W_d^*)'$  is a  $d$ -dimensional Brownian motion with correlation matrix  $\rho^*$  independent of  $W$ . We impose a sparse structure on  $\rho^*$ , which naturally renders a sparse structure of the integrated idiosyncratic volatility matrix

$$\Sigma^e = (\Sigma_{im}^e)_{d \times d} = \left( \int_0^T \sigma_{is}^* \rho_{im}^* \sigma_{ms}^* ds \right)_{d \times d}.$$

**Assumption 3.** The correlation matrix  $\rho^*$  belongs to  $\mathcal{I}_q(m_d) = \left\{ \rho^* : \max_m \sum_{i=1}^d |\rho_{im}^*|^q \leq m_d \right\}$ , for some  $0 \leq q < 1$ , and  $m_d$  is a function of  $d$ .

Note that  $m_d$  may be bounded or may slowly diverging to infinity. When  $q = 0$ , Assumption 3 indicates that each asset-specific factor is correlated with at most  $m_d$  assets.

In matrix form, (6) can be rewritten as

$$dY_t = \mu_t dt + \sigma_t dW_t + \sigma_t^* dW_t^*,$$

where  $Y_t = (Y_{1t}, \dots, Y_{dt})'$ ,  $\mu_t = (\mu_{1t}, \dots, \mu_{dt})'$ ,  $\sigma_t^* = \text{diag}(\sigma_{1t}^*, \dots, \sigma_{dt}^*)$  and  $\sigma_t = (\sigma_{it}^l)_{i=1, \dots, d}^{l=1, \dots, r}$  is a  $d \times r$  systematic volatility matrix.

We first give some regularity assumptions on the coefficient processes of  $Y$ . This is commonly used in the literature, e.g., Jacod and Todorov (2014) for univariate models, and Wang and Zou (2010), Fan et al. (2012), Kim et al. (2018), and Kong (2018) for large-dimensional Itô semi-martingales.

**Assumption 4.** There is a sequence  $\tau_m$  of stopping times increasing to infinity, and a sequence  $\varsigma_m$  of bounded positive numbers satisfying, for all  $i = 1, \dots, d$  and  $l = 1, \dots, r$ :

1. (Locally boundedness) when  $t < \tau_m$ ,  $|Z_t| \leq \varsigma_m$  is satisfied for  $Z = \mu_i, \sigma_i^l$ , and  $\sigma_i^*$ ;
2. (Continuity) for  $Z = \sigma_i^l, \sigma_i^*$ ,  $|Z_{t+s} - Z_t|^2 \leq \varsigma_m s^{1-\epsilon}$  for  $\epsilon > 0$ , and  $|E_{\mathcal{F}_{t \wedge \tau_m}}(Z_{(t+s) \wedge \tau_m} - Z_{t \wedge \tau_m})| + |E_{\mathcal{F}_{t \wedge \tau_m}}(Z_{(t+s) \wedge \tau_m} - Z_{t \wedge \tau_m})^2| \leq \varsigma_m s$ .

The last regularity condition holds for  $\sigma_i^l$  and  $\sigma_i^*$  when they follow a Brownian Itô process with locally bounded coefficient processes, which can be verified using the Lévy's continuity theorem.

**Assumption 5.** There exists a sequence of stopping times  $\tau_m \rightarrow \infty$  as well as a sequence of constants  $\varsigma_m^*$  that satisfy:

$$\inf_{0 \leq t \leq \tau_m} \lambda_{\min} \left( \frac{\sigma_t' \sigma_t}{d} \right) \geq \varsigma_m^*, \quad \inf_{0 \leq t \leq \tau_m} \lambda_{\min} \left( \left( \frac{\sigma_t' \sigma_t}{d} \right) \circ \mathcal{P}_t \right) \geq \varsigma_m^*,$$

where  $\mathcal{P}_t = \left( 1 - \frac{p_{it} + p_{mt} - 2p_{it}p_{mt}}{1 - p_{it}p_{mt}} \mathbf{1}_{\{i \neq m\}} \right)_{d \times d}$  is a symmetric matrix. Moreover, for all  $t \in [0, T]$ ,  $\sigma_t' \sigma_t / d$  and  $(\sigma_t' \sigma_t) \circ \mathcal{P}_t / d$  almost surely has distinct eigenvalues and (sorted in decreasing order)



$$\inf_{0 \leq t \leq \tau_m} \min_{1 \leq l \leq r-1} \left| \lambda_{l+1} \left( \frac{\sigma_t' \sigma_t}{d} \right) - \lambda_l \left( \frac{\sigma_t' \sigma_t}{d} \right) \right| \geq \varsigma_m^*,$$

$$\inf_{0 \leq t \leq \tau_m} \min_{1 \leq l \leq r-1} \left| \lambda_{l+1} \left( \left( \frac{\sigma_t' \sigma_t}{d} \right) \circ \mathcal{P}_t \right) - \lambda_l \left( \left( \frac{\sigma_t' \sigma_t}{d} \right) \circ \mathcal{P}_t \right) \right| \geq \varsigma_m^*.$$

Finally, we assume that  $\text{rank} \left( \frac{\sigma_t' \sigma_t}{d} \right) = \text{rank} \left( \left( \frac{\sigma_t' \sigma_t}{d} \right) \circ \mathcal{P}_t \right) = r$ .

Assumption 5 assumes that all leading  $r$  eigenvalues are simple and do not cross during  $[0, T]$ . This setting excludes duplicate eigenvalues. Statistical properties regarding the eigenvalues of the sample covariance matrix can be seen in Hu et al. (2019). The eigenvalue gaps in Assumption 5 guarantee the validity of the  $SIN(\theta)$  theorem, see Fan et al. (2013). Furthermore, Assumption 5 implies that these factors are strong factors, and hence the resulting volatility matrix of the diffusion system is strongly spiked. The weak factor setting is interesting but is not the focus of this article; its corresponding weak factor generalization is left for the future. The setting of the same rank ensures the stability of the factor space.

Next, we assume the weakly dependent structure of  $W^*$ , by constraining the  $L_1$  norm of the correlation coefficient matrix  $\rho^*$ .

**Assumption 6.**  $\sum_{i,j=1}^d |\rho_{ij}^*|/d < C$ .

### 3.2 Estimation of Efficient Price (Co)Volatilities

It remains uncertain whether conventional volatility estimates are biased due to price staleness? how to correct any potential bias? and the extent to which such corrections might impact precision? To this end, we first briefly review the LPCA method and the estimation of systematic and idiosyncratic volatility matrices. Under the efficient price processes  $Y$  (model (6)), the spot systematic and idiosyncratic volatility matrices are defined, respectively, as

$$V_s^c := \sigma_s \sigma_s' \quad \text{and} \quad V_s^e := \sigma_s^* \rho^* \sigma_s^{*'}.$$

The integrated systematic and idiosyncratic co-volatilities are

$$\Sigma_{ij}^c = \int_0^T V_{ij}^c(s) ds \quad \text{and} \quad \Sigma_{ij}^e = \int_0^T V_{ij}^e(s) ds,$$

respectively, where  $V_{ij}^c(s)$  and  $V_{ij}^e(s)$  are the  $(i, j)$ th entry of  $V_s^c$  and  $V_s^e$ , respectively.

Let  $\Delta_j^n Y_i = Y_{it_j} - Y_{it_{j-1}}$ ,  $\delta_s = (\Delta_{[\frac{s}{\Delta_n} + j]}^n Y_i / \sqrt{\Delta_n})_{i=1, \dots, d}^{j=1, \dots, k_n} \equiv (\delta_{ij}^s)_{d \times k_n}$ , which is a  $d \times k_n$  matrix. Here  $\lceil x \rceil$  denotes the smallest integer greater than or equal to  $x$ . The drift is

represented by  $\mu_s = (\mu_{it_{\lceil \frac{s}{\Delta_n} + j \rceil}})_{i=1, \dots, d}^{j=1, \dots, k_n}$ , which is also a  $d \times k_n$  matrix. The matrix  $F_s = (\Delta_{\lceil \frac{s}{\Delta_n} + j \rceil}^n W^l / \sqrt{\Delta_n})_{l=1, \dots, r}^{j=1, \dots, k_n} \equiv (F_s(1), \dots, F_s(k_n))$  is of size  $r \times k_n$ , while  $F_s^* = (\Delta_{\lceil \frac{s}{\Delta_n} + j \rceil}^n W_i^* / \sqrt{\Delta_n})_{i=1, \dots, d}^{j=1, \dots, k_n} \equiv (F_s^*(1), \dots, F_s^*(k_n))$  is a  $d \times k_n$  matrix. The volatility matrix is denoted as  $\sigma_s = (\sigma_{is}^l)_{i=1, \dots, d}^{l=1, \dots, r}$ , resulting in a  $d \times r$  matrix, and  $\sigma_s^* = \text{diag}\{\sigma_{1s}, \dots, \sigma_{ds}\}$  is a  $d \times d$  matrix. Then as  $k_n \Delta_n \rightarrow 0$ , we expect that

$$\delta_s \approx \mu_s \sqrt{\Delta_n} + \sigma_s F_s + \sigma_s^* F_s^*, \quad (7)$$

and we define  $\bar{\delta}_s = \sigma_s F_s + \sigma_s^* F_s^*$ . The discretization error in (7) was shown to be negligible, and the right-hand side of (7) is a discrete approximate factor model. By using PCA in each block, we can then estimate local factors and their loadings. For the local window size  $k_n$ , we assume the following.

**Assumption 7.**  $k_n/\sqrt{n}$  is bounded,  $\log d = o(n^{1/2-\epsilon})$  and  $n/d^{2\delta'} = o(1)$  for some  $\delta' \geq 1$  and any  $\epsilon > 0$ .

Following Kong (2018), in a local window  $(s, \lceil \frac{s}{\Delta_n} \rceil \Delta_n + k_n \Delta_n)$ , PCA is performed on  $\frac{\delta'_s \delta_s}{dk_n}$ . Specifically,  $\hat{F}_s$  is the eigenvector of  $\frac{\delta'_s \delta_s}{dk_n}$  (eigenvalues are sorted in decreasing order) times  $\sqrt{k_n}$  and  $\hat{\sigma}_s \equiv \frac{\delta'_s \hat{F}'_s}{k_n}$ . Then the estimators of  $V_{im}^c(s)$ ,  $V_{ii}^e(s)$ ,  $V_{im}^e(s)$ ,  $\Sigma_{im}^c$ , and  $\Sigma_{im}^e$  are, respectively, given by

$$\begin{aligned} \hat{V}_{im}^c(s) &= \hat{\sigma}'_{is} \hat{\sigma}_{ms}, & \hat{V}_{ii}^e(s) &= \frac{1}{k_n} \sum_{j=1}^{k_n} (\delta_{ij}^s)^2 - \hat{V}_{ii}^c(s), \\ \hat{V}_{im}^e(s) &= \frac{1}{k_n} \sum_{j=1}^{k_n} (\delta_{ij}^s - \hat{\sigma}'_{is} \hat{F}_s(j)) (\delta_{mj}^s - \hat{\sigma}'_{ms} \hat{F}_s(j)) \quad \text{for } i \neq m, \\ \hat{\Sigma}_{im}^c &= k_n \Delta_n \sum_{k=1}^{\lfloor n/k_n \rfloor} \hat{V}_{im}^c(t_{(k-1)k_n}), & \hat{\Sigma}_{im}^e &= k_n \Delta_n \sum_{k=1}^{\lfloor n/k_n \rfloor} \hat{V}_{im}^e(t_{(k-1)k_n}). \end{aligned} \quad (8)$$

For this low-rank plus sparse structure, we use the Principal Orthogonal complement Thresholding (POET) method for the sparse structure, see Fan et al. (2013) and Kong (2018). Taking the spot volatility as an example, we have

$$\hat{V}_s^{eT} = (\hat{V}_{im}^{eT}(s))_{d \times d} \quad \text{with} \quad \hat{V}_{im}^{eT}(s) = \begin{cases} \hat{V}_{ii}^e(s), & i = m, \\ s_{im}(\hat{V}_{im}^e(s)), & i \neq m, \end{cases}$$

where  $s_{im}(\cdot)$  is a generalized shrinkage function (Cai and Liu 2011; Fan et al. 2013) that satisfies the following conditions: (i)  $|s_{im}(z)| \leq c|y|$  for all  $z, y$  satisfying  $|z - y| \leq \tau_{im}$  and some constant  $c > 0$ ; (ii)  $s_{im}(z) = 0$  for  $|z| < \tau_{im}$ ; (iii)  $|s_{im}(z) - z| \leq \tau_{im}$  for all  $z \in \mathbb{R}$ . These conditions

are satisfied by several functions, including the hard thresholding function  $s_{im}(z) = z\mathbb{1}_{\{|z| \geq \tau_{im}\}}$ , the soft thresholding function  $s_{im}(z) = \text{sgn}(z)(|z| - \tau_{im})_+$  and the adaptive lasso rule  $s_{im}(z) = z(1 - |\tau_{im}/z|^\eta)_+$  with  $\eta \geq 1$ . The integrated idiosyncratic volatility is treated analogously and is denoted as  $\hat{\Sigma}^{e\mathcal{T}} = (\hat{\Sigma}_{im}^{e\mathcal{T}})_{d \times d}$ . In addition,  $\tau_{im}$  is an entry-dependent threshold, which is  $\tau_{im} = C\varphi_{nd}\sqrt{\hat{h}_{im}}$  for spot volatility and  $\tau_{im} = C\tilde{\varphi}_{nd}\sqrt{\hat{h}_{im}}$  for integrated volatility (see Theorem 3 for  $\tilde{\varphi}_{nd}$  and  $\varphi_{nd}$ ).<sup>4</sup> Our factor-based estimators of the total spot and integrated volatility matrices are, respectively,

$$\hat{V}_s = \hat{V}_s^c + \hat{V}_s^{e\mathcal{T}} \quad \text{and} \quad \hat{\Sigma} = \hat{\Sigma}^c + \hat{\Sigma}^{e\mathcal{T}}.$$

If staleness happens, we observe  $\tilde{Y}$ , and we denote  $\tilde{\delta}_s = (\Delta_{\lceil \frac{s}{\Delta_n} + j \rceil}^n \tilde{Y}_i / \sqrt{\Delta_n})_{i=1, \dots, k_n}^{j=1, \dots, k_n}$ . In a local window  $(s, \lceil \frac{s}{\Delta_n} \rceil \Delta_n + k_n \Delta_n)$ , we denote  $B_{i \lceil \frac{s}{\Delta_n} \rceil + j} = B_{si}(j) = B_s(i, j)$ ,

$$\alpha_{s,jl}^{(i)} = (1 - B_s(i, j)) \prod_{k=1}^l B_s(i, j - k) \quad \text{for } l \leq 1, \quad \text{and} \quad \alpha_{s,j0}^{(i)} = (1 - B_s(i, j)).$$

Thus, we can express  $\tilde{\delta}_s$  in the following form.

$$\tilde{\delta}_{ij}^s = \Delta_{\lceil \frac{s}{\Delta_n} + j \rceil}^n \tilde{Y}_i / \sqrt{\Delta_n} = \sum_{l=0}^{j-1} \alpha_{s,jl}^{(i)} \Delta_{\lceil \frac{s}{\Delta_n} + j - l \rceil}^n Y_i / \sqrt{\Delta_n} = \sum_{l=1}^j \alpha_{s,j(j-l)}^{(i)} \Delta_{\lceil \frac{s}{\Delta_n} + l \rceil}^n Y_i / \sqrt{\Delta_n},$$

and the relationship between  $\tilde{\delta}_s$  and  $\delta_s$  is  $\tilde{\delta}_{ij}^s = \sum_{l=1}^j \alpha_{s,j(j-l)}^{(i)} \delta_{il}^s$ . The introduction of price staleness in our model is similar to incorporating factor lags. However, our model adds complexity by using random coefficients. To determine the number of factors,  $r$ , we use an information-type approach, minimizing the aggregated mean square residual error with a penalty, as outlined in Kong (2017).

### 3.3 Results of Estimating the Efficient Price (Co)Volatilities

Our first result below demonstrates that ignoring the price staleness causes bias in estimating the covolatilities.

**Theorem 3.** *Suppose Assumptions 1–7 hold,  $\max_{m \leq d} \sum_{i=1}^d |\rho_{im}^*| / \sqrt{d} < C$ ,  $\lambda_{\max}(\rho^* \circ \mathcal{P}_s) < C$  for some positive constant  $C$ .*

(i) *For systematic (co)volatilities,*

---

<sup>4</sup>Note that  $\hat{h}_{im}$  and  $\tilde{h}_{im}$  are chosen similarly to Fan et al. (2013), and we choose  $\hat{h}_{im} = \frac{1}{k_n} \sum_{j=1}^{k_n} [(\delta_{ij}^s - \hat{\sigma}'_{is} \hat{F}_s(j))(\delta_{mj}^s - \hat{\sigma}'_{ms} \hat{F}_s(j)) - \hat{V}_{im}^e(s)]^2$  and  $\tilde{h}_{im} = k_n \Delta_n \sum_{k=1}^{\lfloor n/k_n \rfloor} [\hat{V}_{im}^e(t_{(k-1)k_n}) - \hat{\Sigma}_{im}^e]^2$ .

$$\begin{aligned}\hat{V}_{im}^c(s) - \left(1 - \frac{p_{is} + p_{ms} - 2p_{is}p_{ms}}{1 - p_{is}p_{ms}} \mathbb{1}_{\{i \neq m\}}\right) \sigma'_{is} \sigma_{ms} &= O_P\left(\frac{1}{d \wedge n^{1/4}}\right), \\ \hat{\Sigma}_{im}^c - \int_0^T \left(1 - \frac{p_{is} + p_{ms} - 2p_{is}p_{ms}}{1 - p_{is}p_{ms}} \mathbb{1}_{\{i \neq m\}}\right) \sigma'_{is} \sigma_{ms} ds &= O_P\left(\frac{1}{d \wedge n^{1/2}}\right).\end{aligned}$$

(ii) For idiosyncratic volatility matrices,

$$\begin{aligned}P\left(\sup_{\rho^* \in \mathcal{I}_q(m_d)} \|\hat{V}_{s,\hat{r}}^{e\mathcal{T}} - V_s^{e,(p)}\| \leq C_q m_d \varphi_{nd}^{1-q}\right) &= 1 - O(d^{-\delta'} n^{1/2} + d^{-\delta'/2} + d^{1-\delta'} n^{1-\delta'/2}), \\ P\left(\sup_{\rho^* \in \mathcal{I}_q(m_d)} \|\hat{\Sigma}_{\hat{r}}^{e\mathcal{T}} - \Sigma^{e,(p)}\| \leq C_q m_d \tilde{\varphi}_{nd}^{1-q}\right) &= 1 - O(d^{-\delta'} n^{1/2} + d^{-\delta'/2} + d^{1-\delta'} n^{1-\delta'/2}),\end{aligned}$$

for some constant  $C_q$ , where  $\varphi_{nd} = \frac{1}{\sqrt{d}} + \frac{\sqrt{\log d}}{n^{1/4}}$ ,  $\tilde{\varphi}_{nd} = \frac{1}{\sqrt{d}} + \frac{\sqrt{\log d}}{\sqrt{n}}$ ,  $V_s^{e,(p)} = V_s^e \circ \mathcal{P}_s$  and  $\Sigma^{e,(p)} = \int_0^T V_s^{e,(p)} ds$ .

The process  $p$  do not bias the estimates of both spot and integrated systematic volatilities ( $i = m$ ), but bias the estimates of the co-volatilities ( $i \neq m$ ). Interestingly, our rates of convergence are the same as those for the efficient price volatility estimates given in [Kong \(2018\)](#). Moreover, we find that the  $(i, m)$ th entry of  $\mathcal{P}_s$  equals 0 if either  $p_{is}$  or  $p_{ms}$  reaches 1. In such cases, recovering the effective price covariance matrix is not easy, which is avoided by [Assumption 1.2](#).

[Theorem 3](#) (ii) proves that the threshold estimates of sparse spot and integrated idiosyncratic volatility matrices converge at rates  $m_d \varphi_{nd}^{1-q}$  and  $m_d \tilde{\varphi}_{nd}^{1-q}$ . If  $m_d \varphi_{nd}^{1-q} = o(1)$ ,  $m_d \tilde{\varphi}_{nd}^{1-q} = o(1)$ , and  $d^{-\delta'} n^{1/2} + d^{1-\delta'} n^{1-\delta'/2} = o(1)$ , then  $\hat{V}_{s,\hat{r}}^{e\mathcal{T}}$  and  $\hat{\Sigma}_{\hat{r}}^{e\mathcal{T}}$  are consistent estimates of  $V_s^{e,(p)}$  and  $\Sigma^{e,(p)}$ , respectively. Note that  $V_s^{e,(p)}$  and  $\Sigma^{e,(p)}$  are influenced by  $\mathcal{P}_s$ , indicating that price staleness affects both systematic and idiosyncratic co-volatilities.

One of our main goals is to estimate  $V_s$ , a  $d \times d$  dimensional total volatility matrix. We achieve this using a low-rank plus sparse structure and by imposing a threshold constraint on the idiosyncratic volatility matrix. In cases with highly spiked eigenvalues, covariance matrices cannot be consistently estimated in the spectral norm, but they can be accurately estimated in terms of the relative errors, as discussed by [Fan et al. \(2008\)](#) and [Fan et al. \(2013\)](#). Specifically, we consider the relative error matrix  $V_s^{-1/2} \hat{V}_{s,\hat{r}} V_s^{-1/2} - I_d$ , measured by its normalized Frobenius norm  $d^{-1/2} \|V_s^{-1/2} \hat{V}_{s,\hat{r}} V_s^{-1/2} - I_d\|_F = \|\hat{V}_s - V_s\|_{V_s}$ . The factor  $d^{-1/2}$  is used for normalization. Let  $V_s^{(p)} = V_s \circ \mathcal{P}_s$ . The following theorem summarizes the convergence results of the estimated total volatility matrix and its inverse.

**Theorem 4.** *Assuming the conditions in [Theorem 3](#).*

(i) Let  $\varphi_{nd} = \frac{1}{\sqrt{d}} + \frac{\sqrt{\log d}}{n^{1/4}}$ , for some positive constant  $C_q$ ,

$$\begin{aligned} P \left( \sup_{\rho^* \in \mathcal{I}_q(m_d)} \|\hat{V}_{s,\hat{r}} - V_s^{(p)}\|_{V_s^{(p)}} \leq C_q \left( m_d \varphi_{nd}^{1-q} + \frac{1}{d^{1/4}} + \frac{\sqrt{d \log d}}{n^{(1-\epsilon)/2}} \right) \right) \\ = 1 - O(d^{-\delta'} n^{1/2} + d^{-\delta'/4} + d^{1-\delta'} n^{1-\delta'/2}). \end{aligned}$$

(ii) If  $m_d \varphi_{nd}^{1-q} = o(1)$ ,  $d^{-\delta'} n^{1/2} + d^{1-\delta'} n^{1-\delta'/2} = o(1)$ ,  $\inf_{s \in [0, T]} \min_{1 \leq i \leq d} |\sigma_{is}^*| > c^{-1}$  and  $c^{-1} \leq \lambda_{\min}(\rho^* \circ \mathcal{P}_s) \leq \lambda_{\max}(\rho^* \circ \mathcal{P}_s) \leq c$  for some positive constant  $c$ ,

$$\|(\hat{V}_{s,\hat{r}})^{-1} - (V_s^{(p)})^{-1}\| = O_P \left( m_d \varphi_{nd}^{1-q} + \frac{1}{\sqrt{d}} + \frac{\sqrt{\log d}}{n^{1/4}} \right).$$

In Theorem 4, the term  $\frac{1}{d^{1/4}} + \frac{\sqrt{d \log d}}{n^{(1-\epsilon)/2}}$  arise from the estimation of the common factor. This implies that a larger sample size  $n$  is required when price staleness exists to offset the error introduced by price staleness.

Theorem 4 also indicates that our volatility matrix estimate (precision matrix estimate) is not consistent to the volatility matrix (precision matrix) of the efficient price in the presence of price staleness. As mentioned in Section 3.2, we can correct for systematic and idiosyncratic volatility estimators to obtain unbiased estimators. One straightforward correction for  $i \neq m$  is

$$\begin{aligned} \hat{V}_{im}^{c*}(s) &:= \hat{V}_{im}^c(s) \phi(\hat{p}_{is}, \hat{p}_{ms})^{-1}, \quad \hat{V}_{im}^{e*}(s) := \hat{V}_{im}^e(s) \phi(\hat{p}_{is}, \hat{p}_{ms})^{-1}, \\ \hat{\Sigma}_{im}^{c*} &:= k_n \Delta_n \sum_{k=1}^{\lfloor n/k_n \rfloor} \hat{V}_{im}^c(t_{(k-1)k_n}) \phi(\hat{p}_{it_{(k-1)k_n}}, \hat{p}_{mt_{(k-1)k_n}})^{-1}, \\ \hat{\Sigma}_{im}^{e*} &:= k_n \Delta_n \sum_{k=1}^{\lfloor n/k_n \rfloor} \hat{V}_{im}^e(t_{(k-1)k_n}) \phi(\hat{p}_{it_{(k-1)k_n}}, \hat{p}_{mt_{(k-1)k_n}})^{-1}, \end{aligned}$$

where  $\hat{V}_{im}^c(s)$  and  $\hat{V}_{im}^e(s)$  are obtained from (8), and  $\hat{p}_{is}$  and  $\hat{p}_{ms}$  are obtained from maximum likelihood estimation in (4), and  $\phi(x, y) = \frac{(1-x)(1-y)}{1-xy}$ . Similarly, the idiosyncratic volatility matrix estimators can be corrected as  $\hat{V}_s^{e*\mathcal{T}}$  (spot) and  $\hat{\Sigma}^{e*\mathcal{T}}$  (integrated). Define

$$\hat{V}_s^* = \hat{V}_s^{c*} + \hat{V}_s^{e*\mathcal{T}} \quad \text{and} \quad \hat{\Sigma}^* = \hat{\Sigma}^{c*} + \hat{\Sigma}^{e*\mathcal{T}}.$$

The next theorem gives the convergence rates of the corrected estimators of the systematic and idiosyncratic volatilities.

**Theorem 5.** *Assuming the conditions in Theorem 3 and additional condition  $\lambda_{\max}(\rho^*) < C$*

for some positive constant  $C$ .

(i) For systematic covolatilities with  $i \neq m$ ,

$$\begin{aligned}\hat{V}_{im}^{c*}(s) - \sigma'_{is}\sigma_{ms} &= O_P\left(\frac{1}{d^{1/2} \wedge n^{1/4}}\right), \\ \hat{\Sigma}_{im}^{c*} - \int_0^T \sigma'_{is}\sigma_{ms}ds &= O_P\left(\frac{1}{d^{1/2} \wedge n^{1/2}}\right).\end{aligned}$$

(ii) For idiosyncratic volatility matrices, assume there exist constants  $\delta^\dagger$ ,  $\delta^\ddagger$ , and  $\delta^\S$  such that

$$\frac{d}{n^{1+\delta^\dagger}} + \frac{n}{d^{2-\delta^\ddagger} \log d} + \frac{d}{n^{2-\delta^\S} \log n} = o(1). \text{ Then, for some constant } C_q,$$

$$\begin{aligned}P\left(\sup_{\rho^* \in \mathcal{I}_q(m_d)} \|\hat{V}_{s,\hat{r}}^{e*\mathcal{T}} - V_s^e\| \leq C_q m_d \hat{\varphi}_{nd}^{1-q}\right) &= 1 - O(d^{-\delta'} n^{1/2} + d^{-\delta'/2} + d^{1-\delta'} n^{1-\delta'/2}), \\ P\left(\sup_{\rho^* \in \mathcal{I}_q(m_d)} \|\hat{\Sigma}_{\hat{r}}^{e*\mathcal{T}} - \Sigma^e\| \leq C_q m_d \check{\varphi}_{nd}^{1-q}\right) &= 1 - O(d^{-\delta'} n^{1/2} + d^{-\delta'/2} + d^{1-\delta'} n^{1-\delta'/2}),\end{aligned}$$

$$\text{where } \hat{\varphi}_{nd} = \frac{\sqrt{\log n}}{d^{1/2}} + \frac{\sqrt{\log d}}{n^{1/4}} \text{ and } \check{\varphi}_{nd} = \frac{\sqrt{\log n}}{d^{1/2}} + \frac{\sqrt{\log d}}{\sqrt{n}}.$$

A notable feature after the correction is that the rate of spot systematic volatility (resp., integrated systematic volatility) reaches  $d^{1/2} \wedge n^{1/4}$ -consistency (resp.,  $d^{1/2} \wedge n^{1/2}$ -consistency), which is reduced from  $d$  (uncorrected version) to  $d^{1/2}$  in  $d$ . This indicates that higher data dimensions are necessary for accurate volatility estimation with the corrected volatilities. The factors in the sample size  $n$  of the convergence rates of the integrated estimates are much smaller than those of the spot estimates, validating the aggregation efficiency after nonlinear factor analysis.

After the price staleness correction, the resulting estimates are unbiased, which is true for the total volatility matrix and its inverse.

**Theorem 6.** *Assuming the conditions in Theorem 5.*

(i) Let  $\hat{\varphi}_{nd} = \frac{\sqrt{\log n}}{d^{1/2}} + \frac{\sqrt{\log d}}{n^{1/4}}$ , and for some positive constant  $C_q$ ,

$$\begin{aligned}P\left(\sup_{\rho^* \in \mathcal{I}_q(m_d)} \|\hat{V}_{s,\hat{r}}^* - V_s\|_{V_s} \leq C_q \left(m_d \hat{\varphi}_{nd}^{1-q} + \frac{1}{d^{1/4}} + \frac{\sqrt{d \log d}}{n^{(1-\epsilon)/2}} + \sqrt{\frac{\log n}{d}}\right)\right) \\ = 1 - O(d^{-\delta'} n^{1/2} + d^{-\delta'/4} + d^{1-\delta'} n^{1-\delta'/2}).\end{aligned}$$

(ii) If  $m_d \hat{\varphi}_{nd}^{1-q} = o(1)$ ,  $d^{-\delta'} n^{1/2} + d^{1-\delta'} n^{1-\delta'/2} = o(1)$ ,  $\inf_{s \in [0, T]} \min_{1 \leq i \leq d} |\sigma_{is}^*| > c^{-1}$  and  $c^{-1} \leq \lambda_{\min}(\rho^*) \leq \lambda_{\max}(\rho^*) \leq c$  for some positive constant  $c$ ,

$$\|(\hat{V}_{s,\hat{r}}^*)^{-1} - (V_s)^{-1}\| = O_P \left( m_d \hat{\varphi}_{nd}^{1-q} + \frac{\sqrt{\log n}}{d^{1/2}} + \frac{1}{d^{1/4}} + \frac{\sqrt{\log d}}{n^{1/4}} \right).$$

For the estimation error of the estimated spot volatility, the concentration type inequality implies that  $\sqrt{\log n/d}$  comes from estimating the staleness  $p_t$ . For the precision matrix,  $\sqrt{\log n/d}$  comes from the estimation of  $p_t$  as well. Thus, the introduction of an estimate of  $p_t$  introduces extra errors.

## 4 Simulation

### 4.1 Simulation Design

We generate one-minute or five-minute high-frequency data (6.5 hours per day) from the process

$$\begin{cases} \tilde{Y}_{it_0} = Y_{it_0} = \log(100), \\ \tilde{Y}_{it_j} = (1 - B_{ij}) Y_{it_{j-1}} + B_{ij} \tilde{Y}_{it_{j-1}}, \quad i = 1, \dots, d. \end{cases}$$

where the Bernoulli variates  $B_{ij}$  are generated in steps: (for  $i = 1, \dots, d$ ):

Step 1. Generate uniformly distributed random variates from  $[0, 1]$  100 times:  $b_{i1}, b_{i2}, \dots, b_{i100}$ .

Step 2. Choose the function  $\Psi$  in probit or logit forms and generate the path of  $z$  by

$$z_{it_j} = a'_i x_{it_j} + \gamma'_i g_{t_j}.$$

All elements in  $a_i$  are sampled independently from  $U(0, 6)$  and those in  $\gamma_i$  are sampled independently from  $N(0, 1)$ . For  $i = 1, \dots, d$ . The covariate  $x$  and the factor  $g$  are sampled from the following mean reverting processes:

$$dx_{it} = \kappa_x(\mu_x - x_{it})dt + \sigma_x dW_{it}^x, \quad dg_t = \kappa_g(\mu_g - g_t)dt + \sigma_g dW_{it}^g,$$

where  $\kappa_x$  is an  $r_x$ -vector whose  $l$ th entry is  $1 + l/(10r_x)$ ,  $\mu_x$  is an  $r_x$ -vector whose  $l$ th entry is  $-0.01 + l/(2r_x)$ ,  $\sigma_x$  is an  $r_x$ -vector whose  $l$ th entry is  $0.5 + l/(10r_x)$ ,  $\kappa_g$  is an  $r_g$ -vector whose  $l$ th entry is  $0.5 + 2l/r_g$ ,  $\mu_g$  is an  $r_g$ -vector whose  $l$ th entry is  $-0.03 + l/(2r_g)$ ,  $\sigma_g$  is an  $r_g$ -vector whose  $l$ th entry is  $1 + l/(5r_g)$ . The probability  $p$  is obtained by transforming  $\Psi(z)$ . We simulate  $p$  once.

Step 3. Generate Bernoulli variates from  $B_{ij} = \mathbb{1}_{\{b_{ij} \leq p_{it_j}\}}$ .

For the simulation of the efficient price process  $Y$ , we completely follow [Kong \(2018\)](#)'s setup. We assume that the number of price factors  $r$  is 3. Systematic spot volatility is generated by a square root process,

$$d\left(\sigma_{it}^l\right)^2 = c_{li} \left( a_{li} - \left(\sigma_{it}^l\right)^2 \right) dt + \sigma_{li}^0 \sigma_{it}^l dW_{it}^\sigma, \quad l = 1, \dots, r.$$

We set  $a_{1i} = 0.5 + i/d, a_{2i} = 0.75 + i/d, a_{3i} = 0.6 + i/d, c_{1i} = 0.03 + i/(100d), c_{2i} = 0.05 + i/(100d), c_{3i} = 0.08 + i/(100d), \sigma_{1i}^0 = 0.15 + i/(10d), \sigma_{2i}^0 = \sigma_{3i}^0 = 0.2 + i/(10d)$ . The specific volatility process follows the stochastic differential equation,

$$d\left(\sigma_{it}^*\right)^2 = (0.08 + i/(100d)) \left( 0.25 + i/d - \left(\sigma_{it}^*\right)^2 \right) dt + (0.2 + i/(10d)) \sigma_{it}^* dW_{it}^{\sigma*}.$$

We set the initial values to  $(\sigma_{i0}^1, \sigma_{i0}^2, \sigma_{i0}^3) = (\sqrt{0.04}, \sqrt{0.04}, \sqrt{0.03})$  and  $\sigma_{i0}^* = \sqrt{0.03}$ .

As in [Jacod and Todorov \(2014\)](#) and [Kong \(2018\)](#), we generate efficient prices from

$$dY_{it} = \sigma_{it}^1 dW_s^1 + \dots + \sigma_{it}^r dW_s^r + \sigma_{is}^* dW_{is}^*,$$

where  $W_s^1, \dots, W_{is}^*$  are independent, and  $(W_{it}^\sigma, W_{it}^{\sigma*}, W_s^l, W_{is}^*)$  are independent of each other. The correlation structure  $\rho^*$  satisfies a banded structure, with  $\rho \sim U(0, 0.4)$ , defined as

$$\rho^* = \begin{cases} \rho^{|i-m|} \times \mathbb{1}_{\{|i-m| \leq 5\}}, & i \neq m, \\ 1, & i = m. \end{cases}$$

We repeat the simulations 200 times (denoted as  $M$ ) and set  $d = 100, 150$ , and 200. In our estimation, we first assume the number of factors is known. First, we consider the case when  $n = 1170$ , simulating a dataset with one-minute intervals over 3 days ( $3 \times 6.5 \times 60$ ). We set  $\sqrt{k_n} = 30 \approx \sqrt{1170}$ , resulting in the data set being divided into 39 blocks. Additionally, we consider the case when  $n = 234$ , representing a dataset with five-minute intervals over 3 days ( $3 \times 6.5 \times 12$ ). Here, we set  $\sqrt{k_n} = 15 \approx \sqrt{234}$ , dividing the dataset into 15 blocks.

## 4.2 Simulation Results

To evaluate the accuracy of the estimated number of factors of the staleness factor model, we use the percentage of correct (PC) estimates. We report in [Table 1](#) the accuracy results for estimating the number of staleness factors, the staleness probability  $p_t, \hat{V}_t, \hat{V}_t^{(p)}, \hat{\Sigma},$  and  $\hat{\Sigma}^*$  in



different scenarios. The estimation accuracy is measured in various norms averaged over all time stamps on the trajectory.

**Table 1:** Percentages of correctly (PC) identifying the number of factors, root mean square error (RMSE) of  $p$ , and various norms for volatility matrices.

$d$	PC	RMSE $_p$	Without staleness		With staleness + uncorrection		With staleness + correction	
			$\ \hat{V}_t - V_t\ _{V_s}$	$\ \hat{\Sigma} - \Sigma\ $	$\ \hat{V}_t - V_t^{(p)}\ _{V_t^{(p)}}$	$\ \hat{\Sigma} - \Sigma^{(p)}\ $	$\ \hat{V}_t^* - V_t\ _{V_s}$	$\ \hat{\Sigma}^* - \Sigma\ $
Logit (1 min)								
100	0.915	0.654	0.852	0.009	0.984	0.031	1.021	0.055
150	0.950	0.642	0.832	0.007	0.965	0.025	0.998	0.051
200	0.990	0.631	0.804	0.007	0.922	0.018	0.952	0.042
Logit (5 min)								
100	0.850	0.667	0.961	0.013	1.037	0.034	1.142	0.061
150	0.935	0.652	0.951	0.012	1.001	0.028	1.021	0.058
200	0.965	0.642	0.901	0.010	0.981	0.021	0.986	0.051
Probit (1 min)								
100	0.920	0.641	0.841	0.009	0.972	0.028	0.994	0.051
150	0.975	0.631	0.833	0.008	0.961	0.025	0.952	0.053
200	1.000	0.621	0.811	0.007	0.921	0.019	0.941	0.049
Probit (5 min)								
100	0.885	0.685	0.961	0.013	1.134	0.036	1.189	0.063
150	0.925	0.674	0.921	0.011	1.021	0.034	1.024	0.057
200	0.975	0.661	0.884	0.009	0.992	0.027	0.971	0.045

Table 1 demonstrates that 1) different link functions perform similarly; 2) increasing the sampling frequency and dimensionality improves the estimation accuracy; 3) our correction method provides accurate volatility matrix estimations.

To save space, extra simulation results are provided in the Supplementary Material. It includes comparisons between the estimated trajectory  $p_t$  and the true one, as well as illustrations of the asymptotic normality in Corollaries 1 and 2.

## 5 Empirical Application

To examine staleness and its impact on the volatility matrix estimation, we analyze high-frequency data for 152 stocks from April 2014. These stocks, all are constituents of the S&P 500 index, have trading records throughout the chosen period. The data were downloaded from the Pi-Trading database.

Notably, many stocks do not trade at the opening time of 9:30 am but only start trading a few minutes later. Consequently, we begin our intraday sample at 9:40 am, which yields 76

log returns for 5-minute intervals and 380 log returns for 1-minute intervals.<sup>5</sup> In addition to the price data, we include high-frequency trading volume as the sole covariate, along with the transformation  $\log(\text{volume} + 1)$ . Further details on data selection and cleaning procedures are provided in the Supplementary Appendix.

## 5.1 Estimation Results for SFM

Table 2 summarizes the MLE results for the SFM. We observe that the number of staleness factors is consistently around three.

**Table 2:** Summary of the averaged parameters

	$a$	$\gamma$			$g$			$p$
		1st	2nd	3rd	1st	2nd	3rd	
Logit+5min	-0.138	0.671	-0.073	-0.408	-1.588	-0.245	-0.974	0.154
Probit+5min	-0.091	0.771	0.094	-0.222	-0.555	0.078	-0.588	0.154
Logit+1min	-0.218	0.120	0.169	-0.893	1.004	0.014	-0.871	0.292
Probit+1min	-0.074	0.912	0.123	0.035	0.019	-0.026	-0.001	0.291

*Notes.* This table reports the average estimation results for the staleness factor model in April 2014. The values of  $a$  and  $g$  are averaged across dimensions, with  $g$  also averaged over time, while  $p$  averaged across both dimensions and time. The term “1st”, “2nd”, and “3rd” refer to the estimation results for the first three staleness factors.

It demonstrates that the coefficients for the covariates are consistently negative, aligning with [Bandi et al. \(2020\)](#), who found that zero and near-zero trading volumes lead to more zero returns. For the 5-minute data, the estimated price stale probability is lower than that for the 1-minute data, which is consistent to the empirical findings in Finance. However, the link function had only a minor effect on the estimation, giving almost the same estimates of the price stale probability.

To better understand the dynamics of the staleness factors, Figure 2 shows the time series of the 5-minute frequency staleness factors. Several observations are noteworthy. First, the calendar effects (see the discussion in the Supplementary Appendix for a stylized-curve-shaped pattern) are reflected. Second, calendar effects aside, the staleness factors are time-varying and nonstationary. Factors 1 and 3 display nearly opposite trends, while factor 2 appears to be more stable with a tiny negative trend.

To examine the persistence of the staleness factors, Figure 3 displays the autocorrelation function (ACF) of the staleness factors shown in Figure 2. As intuitively suggested by Figure

<sup>5</sup>While removing calendar effects can be valuable, it can also lead to loss of information. In addition, there is no well-developed method for handling calendar effects on staleness.

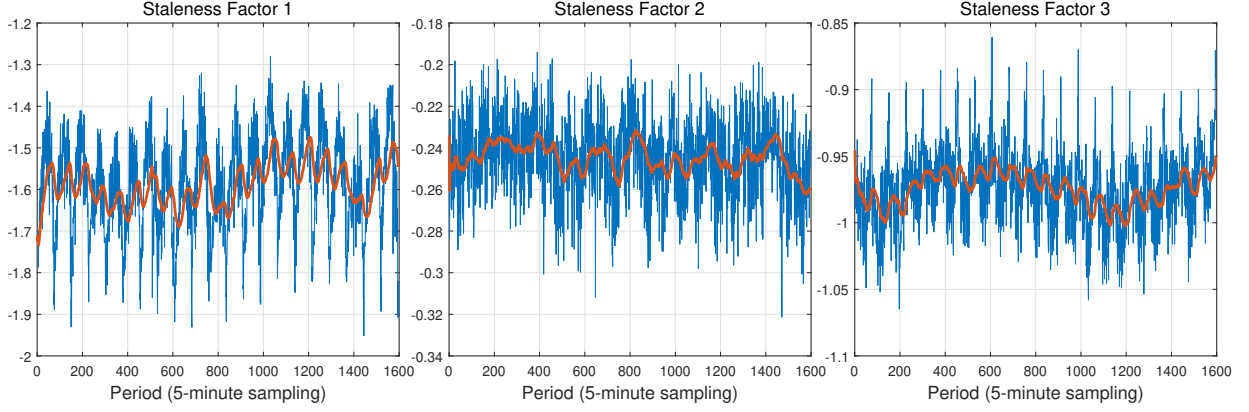


**Figure 2:** Staleness factors. *Notes.* This graph displays the estimated top three staleness factors for April 2014, based on 5-minute sampling intervals. The blue line represents the estimated time series, while the red line shows the 1-day averaged series. A logit-type function is used as the link function.

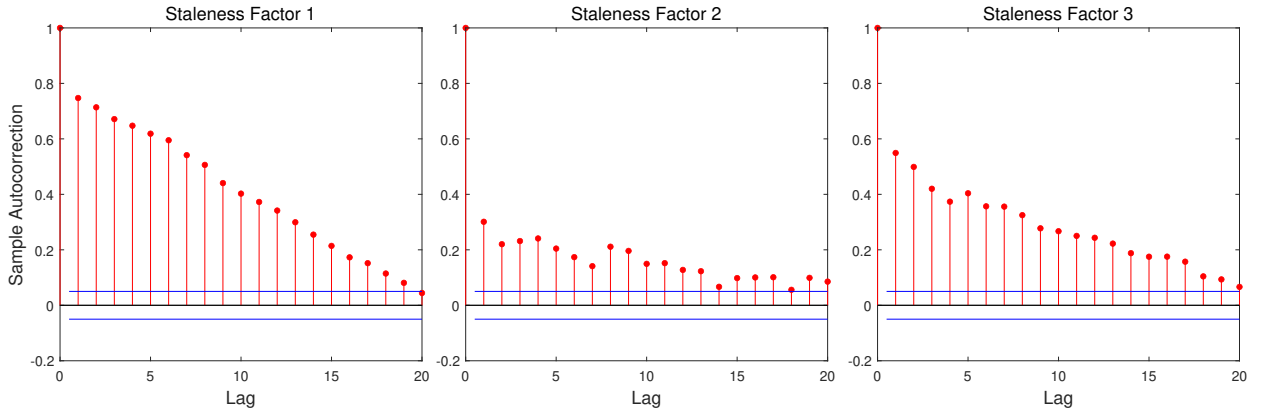


**Figure 3:** Autocorrelation function for the staleness factors. *Notes.* This figure shows the autocorrelation of the top three staleness factors for April 2014, based on 5-minute sampling intervals. The solid blue line represents the 95% confidence level. A logit-type function is used as the link function.

2, all factors exhibit notable persistence, with an ACF extending to about 20 time intervals (5 minutes  $\times$  20  $\approx$  1.7 hours).

## 5.2 Efficient Price Volatility Matrices

To illustrate the impact of staleness on the volatility matrix, Figure 4 shows the changes in the four largest eigenvalues of the spot systematic volatility matrix and the four smallest eigenvalues of the spot idiosyncratic volatility matrix.<sup>6</sup> For idiosyncratic volatility matrix, we use the hard thresholding method.

Our analysis reveals that the eigenvalues of the idiosyncratic volatility are consistently positive, thanks to the POET method. The staleness correction does not significantly change the four smallest eigenvalues of the idiosyncratic volatility matrix (sparse matrix). In contrast, the

<sup>6</sup>We set  $k_n = \lfloor \sqrt{n} \rfloor$  and estimated the number of factor  $r$  by using the LPCA in Kong (2017), resulting in  $\hat{r} = 4$ .

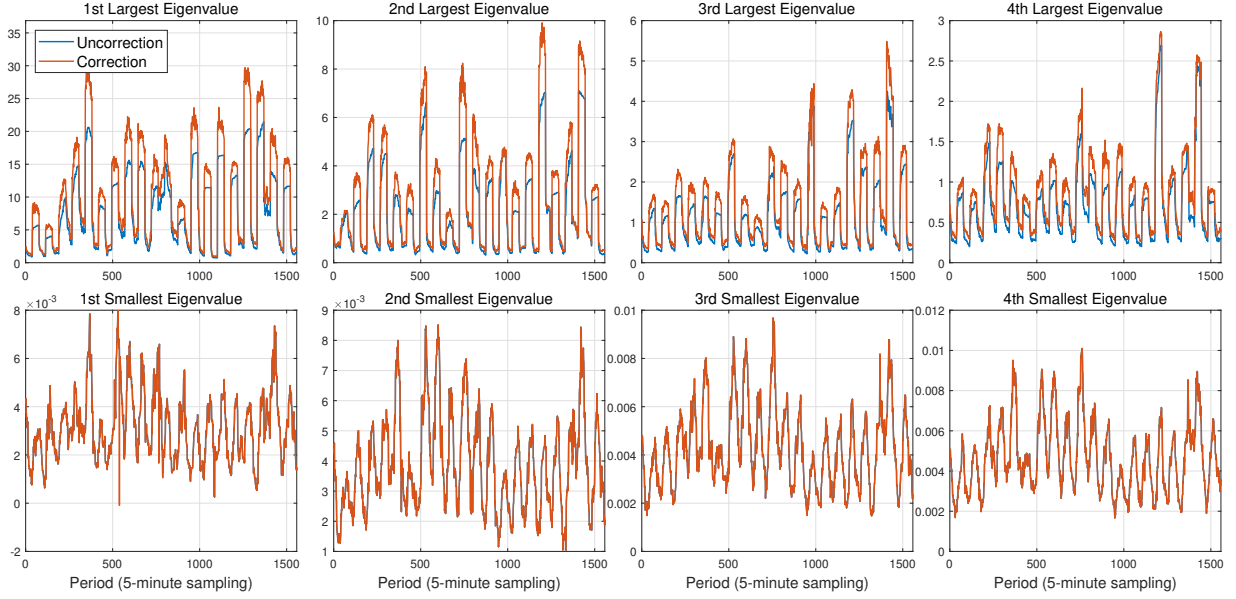


**Figure 4:** Eigenvalues of the spot volatility matrices. *Notes.* This figure displays the four largest eigenvalues of the spot systematic volatility proxies, both uncorrected ( $\hat{V}_s^c$ ) and corrected ( $\hat{V}_s^{c*}$ ) alongside the four smallest eigenvalues of the spot idiosyncratic volatility proxies, both uncorrected ( $\hat{V}_s^e$ ) and corrected ( $\hat{V}_s^{e*\mathcal{T}}$ ). The data, sampled at 5-minute intervals, are from April 2014, with a logit-type function used as the link function.

four largest eigenvalues of the corrected systematic volatility matrix are increased by about 30% after staleness correction, which is consistent to the downward bias in Theorem 3. This finding suggests that routine analyzes such as clustering, principal component analysis, and portfolio allocation—when based on large realized volatility matrices without staleness correction—may yield misleading conclusions.

It is worth noting that Figure 4 also help verify some aspect of Assumption 5. Specifically, the assumption that  $\sigma_t'\sigma_t$  and  $(\sigma_t'\sigma_t) \circ \mathcal{P}_t$  have the same rank is empirically supported. Using the eigen-ratio method to select the number of factors (e.g., Pelger 2019), we observe that the eigen-ratio sequences of  $\sigma_t'\sigma_t$  and  $(\sigma_t'\sigma_t) \circ \mathcal{P}_t$  are almost identical.

### 5.3 Out-of-Sample Portfolio Allocation

We now explore how large-dimensional volatility estimation using high-frequency observations impacts the performance of out-of-sample portfolio allocation. Specifically, we address the following constrained minimum variance portfolio allocation problem (Fan et al. 2012):

$$\min_w w' \widehat{cov} w, \quad \text{subject to} \quad w' \mathbf{1}_d = 1 \text{ and } \|w\|_1 \leq c, \quad (9)$$

where  $c$  represents a risk-exposure constraint bound, with the gross exposure constraint  $c$  varying from 1 to 3, and  $\widehat{cov}$  denotes a working volatility matrix.

When  $c = 1$ , short sales are prohibited, meaning  $\sum_{i=1}^d w_i = 1$  and  $w_i \geq 0$ . When  $c > 1$ ,  $w_i$  can be negative, allowing for short sales. Competing volatility matrices (spot or integrated) are then used to construct the optimal portfolio under a span of exposure constraints. For the month of May 2014, we construct the optimal portfolio based on the volatility matrix estimated from April 2014. This approach assumes that  $\widehat{\text{cov}}_t \approx E_t(\widehat{\text{cov}}_{t+1})$ , a common empirical strategy in practice. To demonstrate the usefulness of staleness correction, we also include the staleness-corrected versions of the volatility matrices.

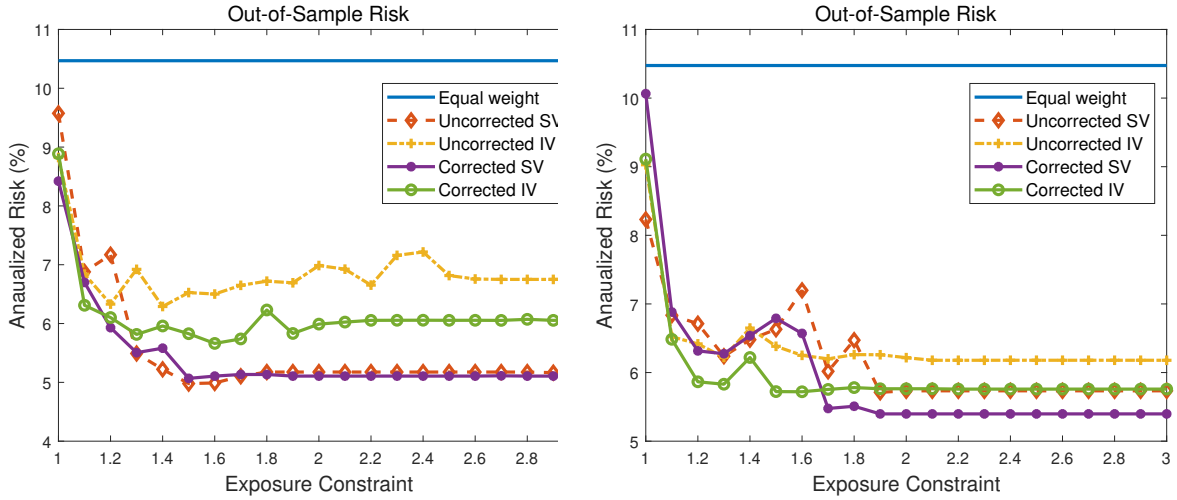


**Figure 5:** Out-of-sample portfolio risk. *Notes.* This figure compares the out-of-sample annualized volatility (for May 2014) of S&P 500 index constituents from April 2014. The left panel presents results using a 5-minute sampling frequency with a logit-type link function, while the right panel uses a 1-minute sampling frequency with a probit-type link function. The x-axis represents the exposure constraint  $c$  in the optimization problem (9). Four volatility matrix estimators are compared: uncorrected spot volatility (Uncorrected SV), uncorrected integrated volatility (Uncorrected IV), corrected spot volatility (Corrected SV), and corrected integrated volatility (Corrected IV). “Equal weight” refers to an equally weighted portfolio.

Figure 5 presents the out-of-sample risks against different risk exposure  $c$ . For comparison, we also construct an equal-weight portfolio, which is independent of the exposure constraints and has an annualized risk of 10.5%.

When  $c = 1$ , the selected optimal no-short-sale portfolios are not well-diversified, resulting in higher out-of-sample annualized risks. As the short-sale constraints are gradually relaxed, the risks for all covariance estimators decrease in trend before they gradually become flat.

Two key findings emerge. 1) Portfolios based on the spot volatility matrix exhibit lower risk compared to those based on the integrated volatility, with or without staleness correction. This might be because spot volatility reflects short-term out-of-sample volatility more accurately, while integrated volatility “averages” the historical volatilities. 2) Volatility matrices corrected for staleness result in relatively lower portfolio risk, pronounced for the integrated volatility,

reducing approximately 10% risk for larger exposure constraint levels.

## 6 Conclusion

This article investigates the cross-sectional dependence of price staleness using a general continuous-time nonlinear nonstationary factor model. We introduce a novel nonstationary maximum likelihood estimation (MLE) procedure and establish the relevant asymptotic theory. We derive a biased downward asymptotic result for the volatility matrix, enabling us to recover and validate the latent effective price volatility matrix. Our method demonstrates good finite sample performance through extensive simulations. The empirical analysis presents relevant estimation results and assesses the impact of staleness on the volatility matrix and its effects on portfolio allocation.

Several avenues for future research are worth exploring. First, while our model assumes constant staleness factor loadings, it would be valuable to extend it to allow for time-varying loadings. This extension is particularly challenging with binary data compared to return/price data. Second, we assume independence between volatility and staleness of effective prices; however, exploring potential correlations between these factors could provide deeper insights. Third, a comprehensive study of price jumps and market microstructure requires simultaneously considering staleness, microstructure noise, and jumps.

In conclusion, staleness plays a critical role in high-frequency theory, comparable to microstructure noise and jumps. This article lays the groundwork for further exploration of staleness in high-dimensional and high-frequency contexts, offering new perspectives and robust tools for asset pricing, risk management and portfolio analysis. Nevertheless, in-depth research remains to be done.

## Supplementary Material

The Supplementary Material contains the proofs of the main theoretical results, additional numerical studies, and more details in the empirical analysis.

## References

- Ait-Sahalia, Y. and D. Xiu (2017). Using principal component analysis to estimate a high dimensional factor model with high-frequency data. *Journal of Econometrics* 201(2), 384–399.
- Bandi, F. M., A. Kolokolov, D. Pirino, and R. Renò (2020). Zeros. *Management Science* 66(8), 3466–3479.
- Bandi, F. M., A. Kolokolov, D. Pirino, and R. Renò (2023). Discontinuous trading in continuous-time econometrics. *Available at SSRN 4351618*.
- Bandi, F. M., D. Pirino, and R. Reno (2017). Excess idle time. *Econometrica* 85(6), 1793–1846.
- Bandi, F. M., D. Pirino, and R. Renò (2024). Systematic staleness. *Journal of Econometrics* 238(1), 105522.
- Cai, T. and W. Liu (2011). Adaptive thresholding for sparse covariance matrix estimation. *Journal of the American Statistical Association* 106(494), 672–684.
- Chen, D. (2024). High frequency principal component analysis based on correlation matrix that is robust to jumps, microstructure noise and asynchronous observation times. *Journal of Econometrics* 240(1), 105701.
- Chen, D., L. Feng, P. A. Mykland, and L. Zhang (2024). High dimensional regression coefficient test with high frequency data. *Journal of Econometrics*, 105812.
- Chen, D., P. A. Mykland, and L. Zhang (2020). The five trolls under the bridge: Principal component analysis with asynchronous and noisy high frequency data. *Journal of the American Statistical Association* 115(532), 1960–1977.
- Dai, C., K. Lu, and D. Xiu (2019). Knowing factors or factor loadings, or neither? Evaluating estimators of large covariance matrices with noisy and asynchronous data. *Journal of Econometrics* 208(1), 43–79.
- Fan, J., Y. Fan, and J. Lv (2008). High dimensional covariance matrix estimation using a factor model. *Journal of Econometrics* 147(1), 186–197.
- Fan, J. and D. Kim (2018). Robust high-dimensional volatility matrix estimation for high-frequency factor model. *Journal of the American Statistical Association* 113(523), 1268–1283.

- Fan, J. and D. Kim (2019). Structured volatility matrix estimation for non-synchronized high-frequency financial data. *Journal of Econometrics* 209(1), 61–78.
- Fan, J., Y. Li, and K. Yu (2012). Vast volatility matrix estimation using high-frequency data for portfolio selection. *Journal of the American Statistical Association* 107(497), 412–428.
- Fan, J., Y. Liao, and M. Mincheva (2013). Large covariance estimation by thresholding principal orthogonal complements. *Journal of the Royal Statistical Society Series B: Statistical Methodology* 75(4), 603–680.
- Gao, J., F. Liu, B. Peng, and Y. Yan (2023). Binary response models for heterogeneous panel data with interactive fixed effects. *Journal of Econometrics* 235(2), 1654–1679.
- Hall, P. and C. C. Heyde (2014). *Martingale limit theory and its application*. Academic press.
- Hu, J., W. Li, Z. Liu, and W. Zhou (2019). High-dimensional covariance matrices in elliptical distributions with application to spherical test. *The Annals of Statistics* 47(1), 527–555.
- Jacod, J. and M. Rosenbaum (2013). Quarticity and other functionals of volatility: Efficient estimation. *The Annals of Statistics* 41(3), 1462–1484.
- Jacod, J. and V. Todorov (2014). Efficient estimation of integrated volatility in presence of infinite variation jumps. *The Annals of Statistics* 42(3), 1029–1069.
- Kim, D., X.-B. Kong, C.-X. Li, and Y. Wang (2018). Adaptive thresholding for large volatility matrix estimation based on high-frequency financial data. *Journal of Econometrics* 203(1), 69–79.
- Kolokolov, A., G. Livieri, and D. Pirino (2020). Statistical inferences for price staleness. *Journal of Econometrics* 218(1), 32–81.
- Kong, X.-B. (2017). On the number of common factors with high-frequency data. *Biometrika* 104(2), 397–410.
- Kong, X.-B. (2018). On the systematic and idiosyncratic volatility with large panel high-frequency data. *The Annals of Statistics* 46(3), 1077–1108.
- Kong, X.-B., J.-G. Lin, C. Liu, and G.-Y. Liu (2023). Discrepancy between global and local principal component analysis on large-panel high-frequency data. *Journal of the American Statistical Association* 118(542), 1333–1344.



- Li, D., O. Linton, and H. Zhang (2024). Estimating factor-based spot volatility matrices with noisy and asynchronous high-frequency data. *arXiv preprint arXiv:2403.06246*.
- Li, J., Y. Liu, and D. Xiu (2019). Efficient estimation of integrated volatility functionals via multiscale jackknife. *The Annals of Statistics* 47(1), 156–176.
- Mancini, C. (2009). Non-parametric threshold estimation for models with stochastic diffusion coefficient and jumps. *Scandinavian Journal of Statistics* 36(2), 270–296.
- Mykland, P. A. and L. Zhang (2009). Inference for continuous semimartingales observed at high frequency. *Econometrica* 77(5), 1403–1445.
- Pelger, M. (2019). Large-dimensional factor modeling based on high-frequency observations. *Journal of Econometrics* 208(1), 23–42.
- Phillips, P. C. and J. Yu (2023). Information loss in volatility measurement with flat price trading. *Empirical Economics* 64(6), 2957–2999.
- Tao, M., Y. Wang, and X. Chen (2013). Fast convergence rates in estimating large volatility matrices using high-frequency financial data. *Econometric Theory* 29(4), 838–856.
- Wang, Y. and J. Zou (2010). Vast volatility matrix estimation for high-frequency financial data. *The Annals of Statistics* 38(2), 943–978.
- Zhu, H. and Z. Liu (2024). On bivariate time-varying price staleness. *Journal of Business & Economic Statistics* 42(1), 229–242.